Earth and Planetary Science Letters 498 (2018) 38–53

Contents lists available at ScienceDirect

Earth and Planetary Science Letters

www.elsevier.com/locate/epsl

The nature and evolution of mantle upwelling at Ross Island, Antarctica, with implications for the source of HIMU lavas

Erin H. Phillips [a,1], Kenneth W.W. Sims [a,*], Janne Blichert-Toft [b], Richard C. Aster [c], Glenn A. Gaetani [d], Philip R. Kyle [e], Paul J. Wallace [f], Daniel J. Rasmussen [g]

[a] Department of Geology and Geophysics, University of Wyoming, 1000 E. University Avenue, Laramie, WY 82071, USA
[b] Laboratoire de Géologie de Lyon, CNRS UMR 5276, Ecole Normale Supérieure de Lyon and Université Claude Bernard Lyon 1, 46 Allée d'Italie, 69007 Lyon, France
[c] Department of Geosciences, Warner College of Natural Resources, Colorado State University, Fort Collins, CO 80523, USA
[d] Department of Geology and Geophysics, Woods Hole Oceanographic Institution, Woods Hole, MA 02543, USA
[e] Department of Earth and Environmental Science, New Mexico Institute of Mining and Technology, Socorro, NM 87801, USA
[f] Department of Earth Sciences, University of Oregon, Eugene, OR 97403, USA
[g] Lamont-Doherty Earth Observatory, Columbia University, Palisades, NY 10964, USA

ARTICLE INFO

Article history:
Received 18 August 2017
Received in revised form 28 May 2018
Accepted 30 May 2018
Available online 2 July 2018
Editor: T.A. Mather

Keywords:
Ross Island
Antarctica
alkaline magmatism
Sr–Nd–Hf–Pb isotopes
mantle upwelling
HIMU

ABSTRACT

The multiple, proximal, young and/or active volcanic centers of Ross Island, Antarctica, provide a unique opportunity to investigate both deep and shallow processes of alkaline magma genesis and the length scales of mantle heterogeneity. Ross Island, Antarctica is an assembly of four silica-undersaturated alkaline volcanic centers, including the active phonolitic Erebus volcano (1.2 to 0 Ma). Mt. Terror, Mt. Bird, and Hut Point Peninsula surround Erebus on the periphery of Ross Island and are mostly older (~0.3 to 4 Ma) and mainly basanitic in composition. While the geochemical compositions and HIMU isotopic signature of Erebus lavas are well characterized, the geochemistry of the peripheral volcanic centers was, until this study, poorly known. To further investigate the nature of mantle sources and magmatic processes beneath Ross Island, we therefore measured major and trace element and Sr, Nd, Hf, and Pb isotope compositions on fifty-seven samples from the three volcanoes peripheral to Erebus volcano and compared the results to previous geochemical and isotopic studies of the latter. Mt. Terror, Mt. Bird, and Hut Point Peninsula have $^{87}Sr/^{86}Sr$ ranging from 0.702907 to 0.703147, ε_{Nd} ranging from +4.3 to +6.3, ε_{Hf} ranging from +5.6 to +8.6, and $^{206}Pb/^{204}Pb$ ranging from 19.282 to 20.241. The Sr, Nd, Hf, and Pb isotope compositions of all four volcanoes (Erebus, Terror, Bird, and Hut Point Peninsula) fall on a mixing line between the HIMU and DMM mantle end-members, with a minor contribution from an EM component. Small, but distinct differences in the isotopic compositions of the four volcanoes, most notably Mt. Bird, imply mantle source heterogeneity beneath Ross Island on a length scale comparable to or smaller than inter-volcano distances (i.e., less than 50 km). The major and trace element systematics and isotopic signatures of the Ross Island volcanic samples are distinct from those for samples from Zealandia and older Antarctic samples that typify magmas from the Cenozoic alkaline magmatic province. The chemical and isotopic compositions of the Ross Island lavas and tephras are best explained by small-degree melting of an ancient asthenospheric source containing residual garnet. Additionally, recent global tomographic modeling indicates low shear wave velocity anomalies with depths down to ~1200 km beneath Ross Island. This suggests a deep-seated upwelling plume impinging on shallower metasomatized mantle which has been gradually eroded away and is no longer a potential source of Ross Island magmatism. Rather, the source of Ross Island lavas is old (Archean to early Proterozoic) material upwelling from the deep mantle as opposed to melting of subcontinental lithospheric mantle metasomatized by Paleozoic subduction. While our findings have local significance in terms of understanding Ross Island volcanism and providing a new perspective on the evolution of volcanism in the surrounding region during the Phanerozoic, they also have important global implications for gauging the nature, age, and evolution of the HIMU mantle source.

* Corresponding author.
E-mail address: ksims7@uwyo.edu (K.W.W. Sims).
[1] Present address: Center for Economic Geology Research, University of Wyoming, 1000 E. University Avenue, Laramie, WY 82071, USA.

https://doi.org/10.1016/j.epsl.2018.05.049
0012-821X/

1. Introduction

Alkaline basalts represent deep, small-degree melts of the mantle. As such, they provide a unique window into some of the mantle's subordinate reservoirs. Here we focus on alkaline HIMU lavas at Ross Island, Antarctica, which is part of a region known as the Cenozoic alkaline magmatic province. It encompasses the easternmost part of the Indo–Australian Plate, the micro-continent of Zealandia, the southwest portion of the Pacific Plate, and West Antarctica (Finn et al., 2005). Finn et al. (2005) used the acronym DAMP for "diffuse alkaline magmatic province" but given that "diffuse" is somewhat vague and this acronym infers a process, we hereinafter prefer to use the more neutral and descriptive "Cenozoic alkaline magmatic province," which refers to a region rather than a process. The Cenozoic alkaline magmatic province is dominantly alkaline, has a widespread "HIMU"-like Pb isotopic signature (e.g., Sun and Hanson, 1975; Hart, 1988; Rocholl et al., 1995; Hart et al., 1995, 1997; Panter et al., 2000, 2006; Rocchi et al., 2002; Finn et al., 2005; Sims and Hart, 2006; Sims et al., 2008), and is generally underlain by low-velocity mantle that extends to depths of ∼600–1450 km (Ritzwoller et al., 2001; Montelli et al., 2006; Nolet et al., 2006; Li et al., 2008; Hansen et al., 2014; French and Romanowicz, 2015; Bozdağ et al., 2016). The Cenozoic alkaline magmatic province also has a complex tectonic history, including subduction along the margin of Gondwana during the Paleozoic–Mesozoic and the Mesozoic break-up of Gondwana (Seton et al., 2012).

While the compositions of the Cenozoic alkaline magmatic province lavas generally are very similar, there are significant geochemical and isotopic distinctions between the region's different volcanic centers (e.g., Timm et al., 2010). These differences likely are a manifestation of the non-uniformity of Phanerozoic tectonic processes across the region. Hence, while it is crucial to recognize the all-encompassing characteristics of the Cenozoic alkaline magmatic province, the details of individual volcanic systems help discern more explicitly relative source contributions and the nature of the processes controlling lava compositions.

An important and well-studied active volcanic system within the Cenozoic alkaline magmatic province is Ross Island in West Antarctica. Ross Island comprises four alkaline volcanic centers: the active, centrally located Erebus volcano and three older (∼0.3–4 Ma) volcanic loci, Mt. Terror, Mt. Bird, and Hut Point Peninsula, which are situated on the periphery of the island (Fig. 1). Erebus, the world's southernmost active volcano, erupts phonolitic lavas from a persistently open magma-filled conduit system, and has been the object of sustained volcanological, geological, and geochemical interest (e.g., Sun and Hanson, 1975; Kyle et al., 1992; Kelly et al., 2008; Sims et al., 2008, 2013; Zandomeneghi et al., 2013; Knox et al., 2018). In contrast, the peripheral Mt. Terror, Mt. Bird, and Hut Point Peninsula volcanoes, which are also silica-undersaturated but primarily composed of primitive basanites, have attracted surprisingly little attention despite their close association with and proximity to Erebus volcano.

A long-standing conceptualization for the magmatic evolution of Ross Island is that it is the expression of a mantle plume (Kyle et al., 1992). The large eruptive volume at Erebus volcano and the presence of kaersutite in the peripheral volcanoes led Kyle et al. (1992) to propose that Ross Island is a concentrically zoned thermal anomaly with the interior being hot asthenospheric upwelling, and the periphery being cooler and incorporating an increased amount of the surrounding asthenosphere and lithosphere. In this model, the peripheral region is represented by the volcanoes Mt. Terror, Mt. Bird, and Hut Point Peninsula, which radially surround Erebus volcano, located in the middle above the center of the thermal anomaly. While the chemical and isotopic compositions of Mt. Erebus are well established (Sims et al., 2008), this is not the case for Mt. Terror, Mt. Bird, and Hut Point Peninsula. Without chemical and isotopic constraints on these volcanoes, the simple concentrically zoned plume hypothesis remains untested.

In order to remedy this shortcoming, and to further advance our understanding of the formation and evolution of Ross Island magmatism, we analyzed major and trace element concentrations and Sr, Nd, Hf, and Pb isotope compositions for 57 volcanic rocks collected from Mt. Terror, Mt. Bird, and Hut Point Peninsula, and compared them to similarly analyzed samples from Erebus volcano (e.g., Sun and Hanson, 1975; Kyle et al., 1992; Sims and Hart, 2006; Kelly et al., 2008; Sims et al., 2008). We further present new geophysical transects extracted from recent deep mantle seismic tomography models (Becker and Boschi, 2002; Simmons et al., 2010; Ritsema et al., 2011; Auer et al., 2014; Chang et al., 2015; French and Romanowicz, 2015) to assess the evidence for a deep plume structure beneath Ross Island and the volcanic provinces of West Antarctica. Our geochemical and isotopic data for Mt. Terror, Mt. Bird, and Hut Point Peninsula, coupled with the existing Erebus data and an improving tomographic resolution of mantle structure in the region, provide for a better understanding of alkaline volcanism on the local scale at Ross Island and also within regional and global contexts.

2. Background

Ross Island is located in the Ross Sea, near the western edge of the Transantarctic Mountains that separate the stable East Antarctic craton from tectonically active West Antarctica (Fig. 1). Lithospheric thickness in East Antarctica is broadly estimated to be >220 km, while in West Antarctica it is ∼70–100 km (Heeszel et al., 2016). Ross Island lies at the southern end of the Terror Rift, which is the locus of the most recent extension within the West Antarctic Rift System (WARS) (e.g., Behrendt, 1999). Ross Island is part of the Erebus volcanic province (Kyle, 1990a), which is a subdivision of the regional McMurdo Volcanic Group (Kyle, 1990b). Crustal thickness beneath the Ross Island region ranges from ∼19 to 25 km (Bannister et al., 2003; Finotello et al., 2011; Chaput et al., 2014). Approximately 4520 km^3 of volcanic rocks have been emplaced on Ross Island since the oldest dated volcanism at ∼4 Ma (Esser et al., 2004).

A simple but complete differentiation sequence from basanite to anorthoclase phonolite is displayed by the Erebus lineage; major crystallizing phases include olivine, clinopyroxene, oxides, feldspar, and apatite (Kyle et al., 1992). Exposed volcanic rocks at Erebus volcano are predominantly anorthoclase-phyric phonotephrite and phonolite (Kyle, 1990a; Kyle et al., 1992; Esser et al., 2004; Kelly et al., 2008). The enriched iron series is a minor lineage of iron-rich lavas on Erebus characterized by Kyle et al. (1992). The oldest dated basanite lavas associated with Erebus are ∼1.3 Ma; the more recent and more evolved anorthoclase-phyric rocks are less than 0.25 Ma (Esser et al., 2004; Parmelee et al., 2015). Lava compositions at Erebus shifted to a largely phonolitic composition at approximately 36 ka (Harpel et al., 2004).

In addition to the Erebus lineage, Ross Island hosts the lineage of the Dry Valley Drilling Project (DVDP), which cored three holes on Hut Point Peninsula in 1973 (Kyle, 1981). Kyle et al. (1992) modeled the evolution of the Erebus and DVDP lineages as originating from a similar basanite parent and evolving along different trends. DVDP and Erebus lineage mineralogies are comparable except that the DVDP lineage also includes kaersutite. The presence of kaersutite reflects wetter conditions and slightly lower temperatures which is a function of different degassing conditions in the peripheral volcanoes as compared to Erebus (Iacovino et al., 2016; Rasmussen et al., 2017). The three peripheral volcanic centers belong to the DVDP lineage; their eruptive products lack modern

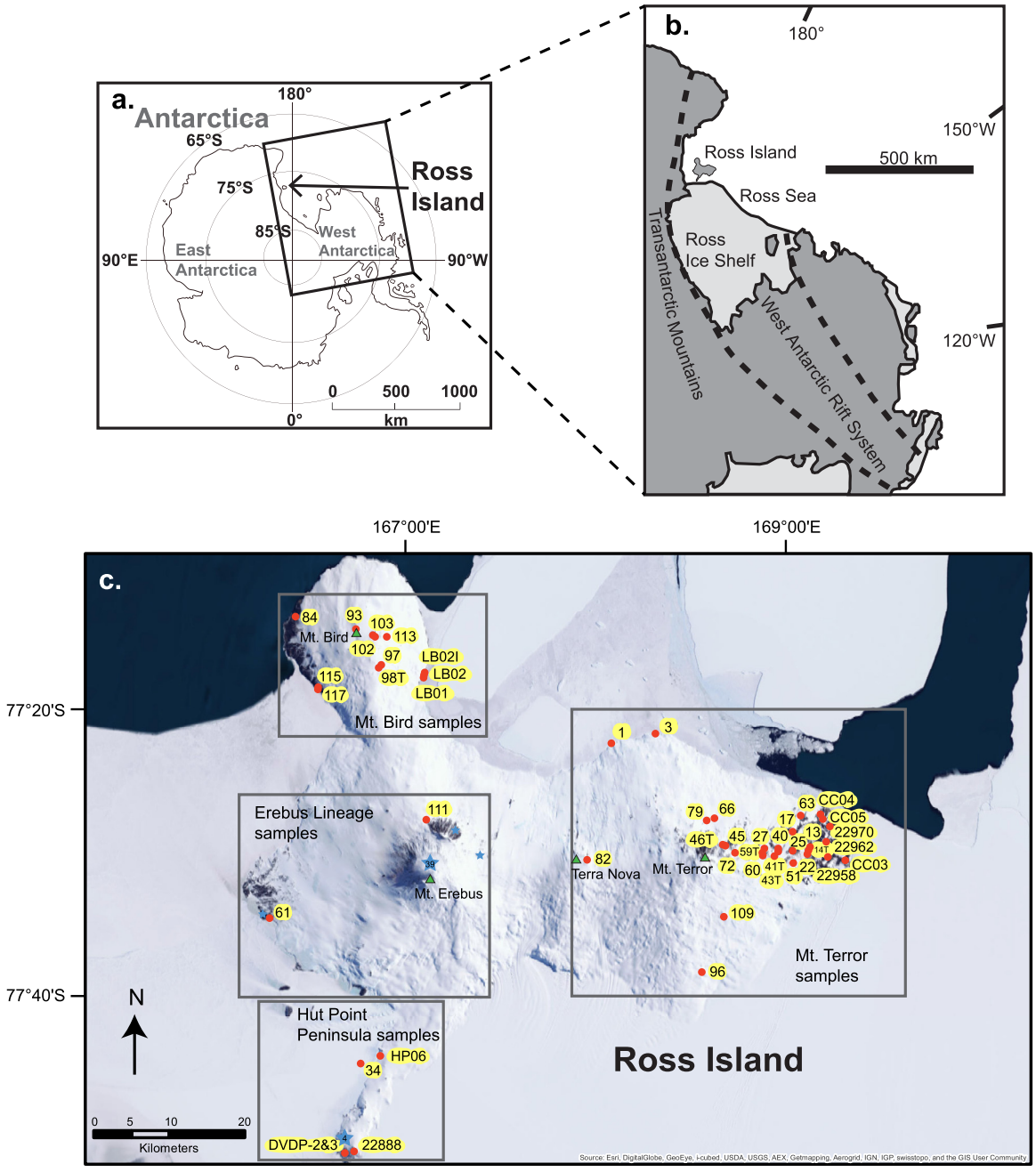

Fig. 1. (a) Map of Antarctica. (b) Map of the West Antarctic Rift System, the Transantarctic Mountains, and Ross Island. (c) Map of Ross Island. Locations of new samples are shown with red circles and sample numbers are highlighted in yellow; "RI" precedes sample numbers 1 through 117; "T" denotes tephra. Dry Valley Drilling Project (DVDP) holes 2 and 3 were drilled in the same location; sample numbers for Hut Point lavas from these drill holes are preceded by 2- or 3- based on the hole from which they were collected. Locations of samples reported by Sims et al. (2008) are shown with blue stars; 39 of these samples are from Erebus crater or summit area and four are from DVDP hole 2; samples from the enriched iron series reported by Sims et al. (2008) are neither shown nor used in comparison with data for Erebus because they show clear signs of crustal contamination. Mt. Erebus, Mt. Terror, Mt. Bird, and Terra Nova are marked by green triangles. Dark gray boxes enclose samples from each of the volcanic centers (Erebus volcano, Mt. Terror, Mt. Bird, and Hut Point Peninsula). See Supplement A for GPS coordinates of samples from this study. (For interpretation of the colors in the figure(s), the reader is referred to the web version of this article.)

high-precision age dates, but they are mostly older than Erebus eruptive products and their lavas generally less evolved than at Erebus volcano. Mt. Terror is a stratovolcano to the east of Erebus volcano with eruptive products between ~0.5 and 2 Ma in age (Armstrong, 1978). Mt. Bird is a shield volcano to the northwest of Erebus volcano with eruptive products ranging in age from ~3 to 4 Ma (Armstrong, 1978). Hut Point Peninsula, located to the south of Erebus volcano, is a 20 km long linear trend of small volcanic centers that appeared between ~0.3 and 1.5 Ma (Kyle, 1981, 1990a).

3. Samples and analytical methods

Ross Island lava and tephra samples were collected in 2012 and 2014 (Supplement A). For complete coverage, select archived samples from Cape Crozier (Cole et al., 1971) and Hut Point Peninsula, including the DVDP core (Kyle, 1981), were included in the sample suite to be analyzed for major and trace element abundances and long-lived radiogenic Sr, Nd, Hf, and Pb isotope compositions. The data from this study are compared to existing data of a large suite of Erebus samples (Sims and Hart, 2006; Sims et al., 2008).

Table 1
Locations and Sr, Nd, Hf, and Pb isotope compositions of selected Ross Island samples. See Supplement A for complete table of results.

Sample	Location	$^{87}Sr/^{86}Sr$	$^{143}Nd/^{144}Nd$	ε_{Nd}	$^{176}Hf/^{177}Hf$	ε_{Hf}	$^{206}Pb/^{204}Pb$	$^{207}Pb/^{204}Pb$	$^{208}Pb/^{204}Pb$
Mt. Terror									
RI 3	77°21′59″S 168°19′38″E	0.703133 ± 9	0.512897 ± 4	5.0	0.282991 ± 5	7.7	19.7659	15.6401	39.3475
RI 14T	77°29′56″S 169°08′34″E	0.703098 ± 8	0.512901 ± 5	5.1	0.282979 ± 4	7.3	19.7038	15.6395	39.2722
RI 25	77°30′07″S 169°03′15″E	0.703119 ± 8	0.512907 ± 4	5.3	0.282971 ± 5	7.0	19.7009	15.6430	39.2787
			0.512922 ± 6[e]	5.5					
RI 45	77°29′53″S 168°42′33″E	0.703069 ± 7	0.512919 ± 5	5.5	0.282998 ± 4	8.0	19.6632	15.6298	39.2056
RI 59T	77°30′22″S 168°51′18″E	0.703041 ± 10	0.512926 ± 6	5.6	0.283008 ± 3	8.3	19.5820	15.6280	39.1661
RI 60	77°30′23″S 168°51′19″E	0.702969 ± 9	0.512942 ± 5	5.9	0.283003 ± 5	8.2	19.5679	15.6189	39.1097
			0.512938 ± 4[e]	5.9					
RI 82	77°30′51″S 167°57′46″E	0.702907 ± 9	0.512959 ± 3	6.3	0.283013 ± 5	8.5	19.4578	15.6055	38.9735
CC 03	77°30′46″S 169°19′56″E	0.703048 ± 7	0.512920 ± 4	5.5	0.282980 ± 6	7.4	19.6812	15.6309	39.2126
22962[a]	77°29′50″S 169°14′02″E	0.703088 ± 10	0.512911 ± 4	5.3	0.282975 ± 6	7.2	19.2820	15.6127	38.8590
			0.512908 ± 4[e]	5.3					
Mt. Bird									
RI 93	77°14′49″S 166°44′45″E	0.702932 ± 12	0.512896 ± 4	5.0	0.283002 ± 4	8.1	19.6796	15.6266	39.4553
RI 98T	77°17′28″S 166°52′03″E	0.703065 ± 9	0.512858 ± 4	4.3	0.282981 ± 5	7.4	19.8412	15.6363	39.7039
RI 117	~77°19′01″S ~166°32′23″E	0.703156 ± 11[d]	0.512898 ± 4	5.1	0.282943 ± 4	6.0	19.7376	15.6244	39.4391
		0.703139 ± 8[d]	0.512897 ± 4[e]	5.1					
LB 02	77°18′04″S 167°06′10″E	0.703126 ± 7	0.512872 ± 5	4.6	0.282983 ± 4	7.5	19.8001	15.6329	39.6306
Hut Point Peninsula[b]									
RI 34	~77°44′39″S ~166°46′01″E	0.703083 ± 11	0.512895 ± 4	5.0	0.282957 ± 5	6.5	19.8778	15.6472	39.4490
			0.512901 ± 5[e]	5.1					
2-45.86[a]	DVDP-2	0.703035 ± 7	0.512889 ± 6	4.9	0.282939 ± 3	5.9	19.8597	15.6498	39.4383
2-105.53[a]	DVDP-2	0.702996 ± 10	0.512919 ± 6	5.5	0.282955 ± 4	6.5	19.7861	15.6393	39.2850
3-267.38	DVDP-3	0.702969 ± 7	0.512904 ± 4	5.2	0.282955 ± 5	6.5	20.0773	15.6488	39.6953
			0.512888 ± 4[e]	4.9					
3-306.33	DVDP-3	0.702972 ± 8	0.512905 ± 3	5.2	0.282956 ± 4	6.5	20.1309	15.6648	39.7147
3-372.27	DVDP-3	0.702991 ± 10	0.512905 ± 3	5.2	0.282951 ± 6	6.3	20.1292	15.6613	39.7235
			0.512898 ± 5[e]	5.1					
22888[a]	77°50′48″S 166°41′59″E	0.703051 ± 7	0.512889 ± 5	4.9	0.282942 ± 5	6.0	20.2406	15.6679	39.7960
Standard[c]									
BCR-2 (unleached)		0.705002 ± 11	0.512632 ± 5	−0.1	0.282871 ± 4	3.5	18.7502	15.6229	38.7251
		0.704999 ± 11	0.512637 ± 5	0.0					
		0.705013 ± 9	0.512630 ± 5	−0.2					
		0.705012 ± 8							

Footnotes (See Supplements A and D for complete footnotes and analytical methods):
[a] Archived powders ground in a tungsten-carbide (WC) shatterbox were used for isotopic analysis for these samples; no W or Ta interferences were observed during Hf isotope analysis. All other samples were ground in a ceramic shatterbox.
[b] Hut Point sample names that are preceded by 2- or 3- are from the DVDP drill core. The DVDP-2 and DVDP-3 holes were located within 2 m of each other at 77°50′53″S, 166°40′53″E.
[c] Measurements of the BCR-2 rock standard that was purified and analyzed along with the Ross Island samples. Multiple listings are analyses of a single purified solution. Additional rock standard analyses reported in Supplement A.
[d] Sr measured on two separate dissolutions and chemical purifications. Duplicate analyses agree within analytical error.
[e] Duplicate Nd isotope measurement at ENS Lyon on same solution measured at UW; duplicate measurements agree within analytical error.

Major and trace element concentrations were measured at Michigan State University by X-ray fluorescence (XRF) and inductively coupled plasma mass spectrometry (ICP-MS), respectively (Supplements B and C). Chemical separation of Sr, Nd, Hf, and Pb was carried out at the University of Wyoming (UW) High Precision Isotope Laboratory and the Ecole Normale Supérieure (ENS) in Lyon, France, on the same dissolutions for each sample (Supplement D). Strontium and Nd isotope compositions were measured at UW and Hf and Pb isotope compositions at ENS Lyon (Table 1; Supplement A). Analyses of mineral separates were done at the UW Materials Characterization Laboratory (Supplement E). Tomographic Antarctic images referred to here utilized global velocity models SEMUCB-WM1 (French and Romanowicz, 2015), SGLOBE-rani (Chang et al., 2015), GyPSuM (Simmons et al., 2010), and SMEAN2 (Becker and Boschi, 2002; Simmons et al., 2010; Ritsema et al., 2011; Auer et al., 2014) (Supplement F).

4. Results

4.1. Whole-rock major and trace element geochemistry

The majority of Mt. Terror, Mt. Bird, and Hut Point Peninsula samples analyzed in this study are basanites, with some ranging to phonolites on a total alkali versus silica diagram (Fig. 2). Erebus

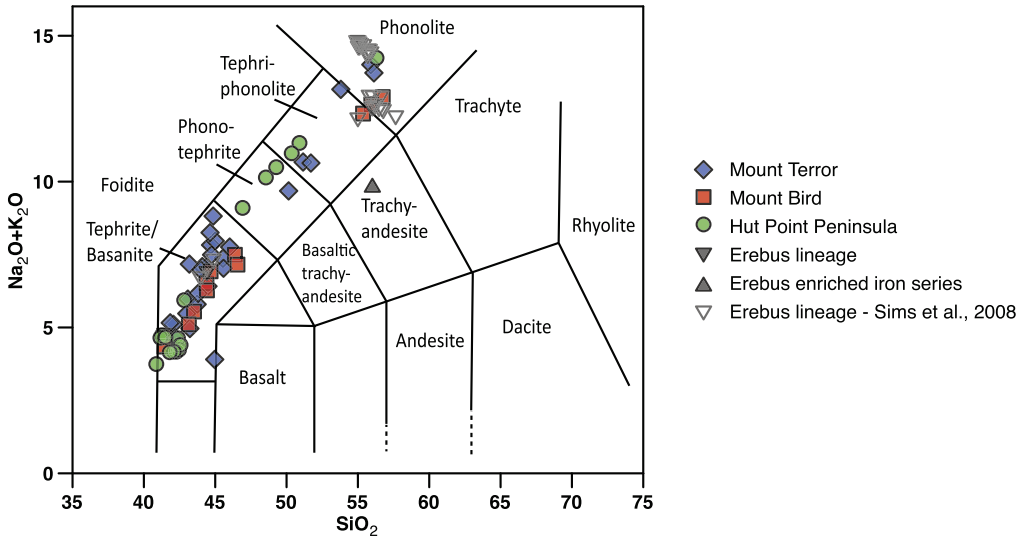

Fig. 2. Total alkalis vs. silica diagram for Ross Island lavas and tephras. Most samples from the peripheral volcanic centers examined in this study are basanites. The Mt. Terror, Mt. Bird, and Hut Point Peninsula samples examined in this study contain SiO_2 ranging from 40.86 to 56.75 wt.% and $Na_2O + K_2O$ ranging from 3.74 to 14.73 wt.%. They range from basanite to phonolite, but the majority of samples plot in the basanite field. MgO ranges from 0.12 to 12.72 wt.%, with an average of 6.43 wt.%. All samples with MgO less than 1 wt.% are phonolites or plot on or close to the phonolite–tephriphonolite divide. Erebus lineage rocks in this study are primarily from anorthoclase phonolite lavas and bombs. Erebus lineage samples plotted from Sims et al. (2008) are those for which there are isotope data, and exclude enriched iron series samples, some of which show clear signs of crustal contamination. The major and trace element data for these samples, including both whole-rock analyses and matrix glass analyses, are presented in Kelly et al. (2008) and Kyle et al. (1992).

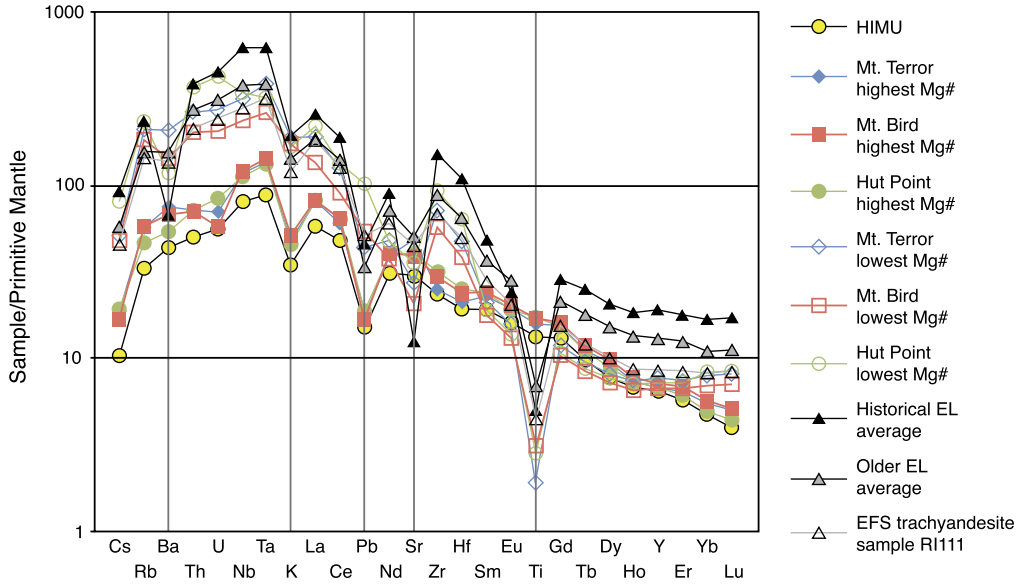

Fig. 3. Primitive mantle-normalized trace element diagram, showing that light REE are enriched over heavy REE in Mt. Terror, Mt. Bird, and Hut Point Peninsula samples, with primitive mantle-normalized La/Yb ranging from 14.5 to 26.2 (see Supplement C). Trace element patterns for the highest Mg# samples from the three peripheral volcanic centers are very similar to each other as well as to the HIMU mantle end-member, with negative K and Pb anomalies. The lowest Mg# samples from Mt. Terror, Mt. Bird, and Hut Point Peninsula show greater enrichments in the most incompatible trace elements, lack significant K and Pb anomalies, and have negative Ti anomalies; these samples more closely resemble Erebus lineage lavas, especially a trachyandesite that likely was affected by crustal contamination. HIMU is an average of 12 samples from St. Helena from Willbold and Stracke (2006). Averages for Erebus volcano are for samples reported in Sims et al. (2008). Major and trace element concentrations for these Erebus samples are reported in Kelly et al. (2008) and Kyle et al. (1992). Historical Erebus lineage (EL) lavas from Kelly et al. (2008) are for matrix glass and older Erebus lineage lavas from Kelly et al. (2008) and Kyle et al. (1992) are for whole-rock samples. Primitive mantle values are from McDonough and Sun (1995). The highest and lowest Mg# samples from Mt. Terror, Mt. Bird, and Hut Point are indicated.

lineage lavas range from basanite to phonolite (Kyle et al., 1992; Sims et al., 2008) with most analyses being on recently erupted phonolite bombs (Kelly et al., 2008; Sims et al., 2008, 2013). MgO concentrations in Mt. Terror, Mt. Bird, and Hut Point Peninsula lavas and tephras range from 0.12 to 12.72 wt.%. Samples with less than 1 wt.% MgO are phonolites or fall along the phonolite-tephriphonolite divide (Fig. 2). Primitive mantle-normalized trace element patterns for volcanic rocks from Ross Island are shown in Fig. 3. The highest Mg# samples all show prominent negative K and Pb anomalies and depletions in Cs and Rb relative to Ba and Th, whereas the lowest Mg# samples lack significant negative K and Pb anomalies and have negative Ti anomalies.

4.2. Long-lived radiogenic isotopes

The Sr, Nd, Hf, and Pb isotope compositions measured on samples from Ross Island include the 57 samples from Mt. Terror (28), Mt. Bird (12), and Hut Point Peninsula (17) mentioned above,

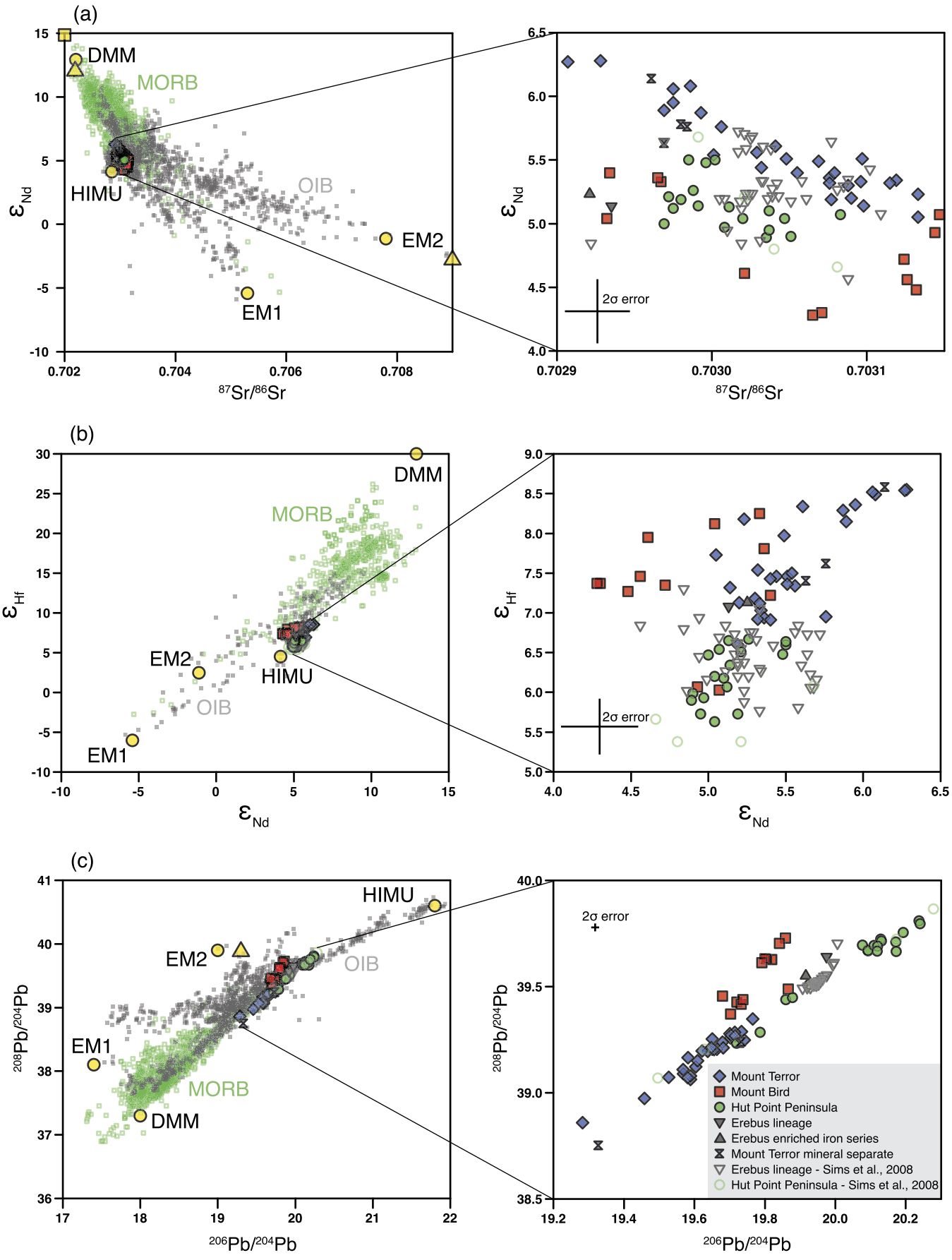
(a)
DMM
MORB
HIMU
OIB
EM2
EM1
ε_{Nd}
$^{87}Sr/^{86}Sr$
2σ error
(b)
DMM
MORB
EM2
HIMU
OIB
EM1
ε_{Hf}
ε_{Nd}
2σ error
(c)
HIMU
EM2
OIB
EM1
MORB
DMM
$^{208}Pb/^{204}Pb$
$^{206}Pb/^{204}Pb$
2σ error
Mount Terror
Mount Bird
Hut Point Peninsula
Erebus lineage
Erebus enriched iron series
Mount Terror mineral separate
Erebus lineage - Sims et al., 2008
Hut Point Peninsula - Sims et al., 2008

as well as one sample from the Erebus lineage at Cape Barne, and one enriched iron series sample from Fang Ridge (Table 1; Supplement A) that were analyzed here to complement existing Erebus data. These are compared with the Sr, Nd, Hf, and Pb isotope compositions of 42 samples from the Erebus lineage and four samples from the DVDP lineage (Sims and Hart, 2006; Sims et al., 2008).

The overall ranges in Sr, Nd, Hf, and Pb isotope compositions for the three peripheral volcanic centers are greater than for the Erebus lineage (Figs. 4–6). On a global scale, all of the Ross Island rocks are isotopically similar to the HIMU mantle end-member in Sr–Nd–Hf–Pb isotope space and plot on a mixing line between the HIMU and depleted mid-ocean ridge basalt (MORB) mantle (DMM) end-members, possibly with a small contribution from an enriched mantle (EM) component (Figs. 4, 5, and 7).

4.3. Mineral separates

To assess the possible presence of xenocrystic material, we analyzed the isotope compositions of four mineral separates from Mt. Terror. The Sr, Nd, Hf, and Pb isotope compositions of the four mineral separates (plagioclase, pyroxene, and two amphiboles) are within the range of whole-rock isotope compositions from Mt. Terror, except for one amphibole that has Pb isotope compositions slightly outside this range (Fig. 4).

5. Discussion

5.1. The significance of isotopic variability at Ross Island

Significant isotopic variability is observed at Ross Island with a general clustering of isotopic compositions within each volcanic center and an overall higher degree of variability within the peripheral volcanic centers relative to the central Erebus volcano (Figs. 4–6). These characteristics point to small-scale mantle source heterogeneities beneath Ross Island on the scale of less than ~50 km (which is the approximate distance between each of the peripheral volcanic centers and Erebus volcano and therefore the smallest scale that can be observed).

The extent to which the observed isotopic variability results from crustal contamination can be evaluated using the relative abundances of key trace elements. Hart et al. (1997) pointed out that negative K and Pb anomalies, along with depletions in Cs and Rb and relatively low $^{87}Sr/^{86}Sr$, are evidence against significant crustal contamination. At Ross Island, samples with different Mg# are characterized by different trace element patterns (Fig. 3). The highest Mg# samples all show prominent negative K and Pb anomalies and depletions in Cs and Rb relative to Ba and Th. These systematics are consistent with the HIMU mantle end-member, indicating a lack of crustal contamination (Fig. 3). Conversely, the lowest Mg# samples lack significant negative K and Pb anomalies and have negative Ti anomalies, suggesting that they have been affected by crustal contamination. Such crustal contamination is particularly evident in the Erebus trachytes of the enriched iron series, which show distinctive isotopic characteristics, namely high $^{87}Sr/^{86}Sr$ and low $^{208}Pb/^{204}Pb$ (Sims et al., 2008).

Given the observed isotopic variability at Ross Island, the evolved nature of some of the samples (Fig. 2) further raises the question of whether shallow differentiation and assimilation have had a systematic effect on the isotope composition of the lavas and tephras. If variations in the isotope compositions at Ross Island were significantly impacted by shallow differentiation (i.e., fractional crystallization) and assimilation of felsic crust, one would expect a correlation between isotope compositions and both Mg# (Supplement G) and trace element ratios such as Nb/La, which is not observed for any of the peripheral volcanic centers. This, therefore, indicates that the isotope compositions are not systematically controlled by assimilation or differentiation processes. Even if only the most primitive samples (Mg# $>$ 50) are considered, the general observation of overall greater compositional variability of the peripheral volcanic centers compared to Erebus volcano and the clustering of isotope compositions for each peripheral volcanic center, indicate small, but analytically significant source variability at Ross Island. Additionally, samples from the peripheral volcanic centers do not have the same isotopic characteristics as the Erebus enriched iron series trachytes, which have been shown unambiguously to have evolved along a different liquid line of descent than the majority of Erebus lineage lavas and to have been affected by significant crustal contamination (Kyle et al., 1992; Sims et al., 2008). Therefore, we conclude that the statistically significant variations in isotope compositions observed at Ross Island are the result of partial melting of a heterogeneous mantle source with assimilation playing a subordinate role only for the more evolved rocks.

These observations provide important insights into the meaning of the isotopic variability across Ross Island (Figs. 4–6). Mt. Terror lavas and tephras have the highest ε_{Nd} and ε_{Hf} and least radiogenic Pb isotope compositions and show a relatively wide range in Sr isotope compositions. Hut Point lavas and tephras are the most similar to Erebus volcano in terms of their Nd and Hf isotope compositions and have the most radiogenic Pb. Mt. Bird shows a range similar to Mt. Terror for its Sr isotope compositions, whereas divergent trends emerge in Nd–Hf–Pb isotope space (Figs. 4b, c). Two samples from the Mt. Bird sea cliffs are outliers when compared to other Mt. Bird samples with respect to their Hf isotope compositions ($\varepsilon_{Hf} = +6.0$ and $+6.1$), suggesting they tapped a slightly different mantle component than the other rocks from Mt. Bird. With the exception of these two cliff lavas, Mt. Bird lavas and tephras exhibit unusually radiogenic Hf isotope compositions for a given Nd isotope composition, resulting in a shallowing of the Nd–Hf trend for Mt. Bird. One potential explanation for this observation is the presence of deep-sea pelagic sediments in the source of Mt. Bird eruptive products, an occurrence first identified by Blichert-Toft et al. (1999) in Hawaiian lavas based on their shallow slope in Nd–Hf isotope space compared to the mean global ocean island basalt (OIB) array. It should be noted, however, that Ross Island rocks display a relatively narrow range in Nd and Hf isotope compositions compared to Hawaii, suggesting only minor influence of pelagic sediments in the source of Mt. Bird eruptive products. We further note that other common indicators of pelagic sediment, such as relatively low Ce/Pb (see e.g., Sims and DePaolo,

Fig. 4. Isotope plots showing the similarity of Ross Island lavas and tephras to OIB and the HIMU mantle end-member, the overall greater variability of the peripheral volcanic centers at Ross Island compared to Erebus volcano, and the general clustering of isotope compositions within each volcanic center. Plots on the left-hand side include MORB in green and OIB in gray. Plots on the right-hand side show Ross Island lavas and tephras in detail. The Sr, Nd, Hf, and Pb isotope data from this study for 28 samples from Mt. Terror, 12 samples from Mt. Bird, 17 samples from Hut Point Peninsula, 1 sample from the Erebus lineage, 1 sample from the Erebus enriched iron series, and 4 mineral separates from the Terror area are presented in Supplement A. Erebus lineage samples from Sims et al. (2008) exclude enriched iron series samples, which show clear signs of crustal contamination. (a) $^{87}Sr/^{86}Sr$ versus ε_{Nd}. Mantle end-members are shown with yellow symbols; depleted MORB mantle (DMM) from Hart et al. (1992; circle), Salters and Stracke (2004; square), and Workman and Hart (2005; triangle); HIMU and enriched mantle 1 (EM1) from Hart et al. (1992); enriched mantle 2 (EM2) from Hart et al. (1992; circle) and Workman et al. (2004; triangle). (b) ε_{Nd} versus ε_{Hf}. Mantle end-members, shown with yellow circles, are inferred for Hf isotope compositions from their Nd isotope compositions in Hart et al. (1992). (c) $^{206}Pb/^{204}Pb$ versus $^{208}Pb/^{204}Pb$. Mantle end-members are shown with yellow symbols; depleted MORB mantle (DMM), HIMU, and enriched mantle 1 (EM1) from Hart et al. (1992; circles); enriched mantle 2 (EM2) from Hart et al. (1992; circle) and Workman et al. (2004; triangle). Error bars shown are 2σ external precision based on replicate measurements of standards (see Supplements A and D). The isotope compositions of the Ross Island lavas and tephras plot on a mixing line between the HIMU and DMM end-members.

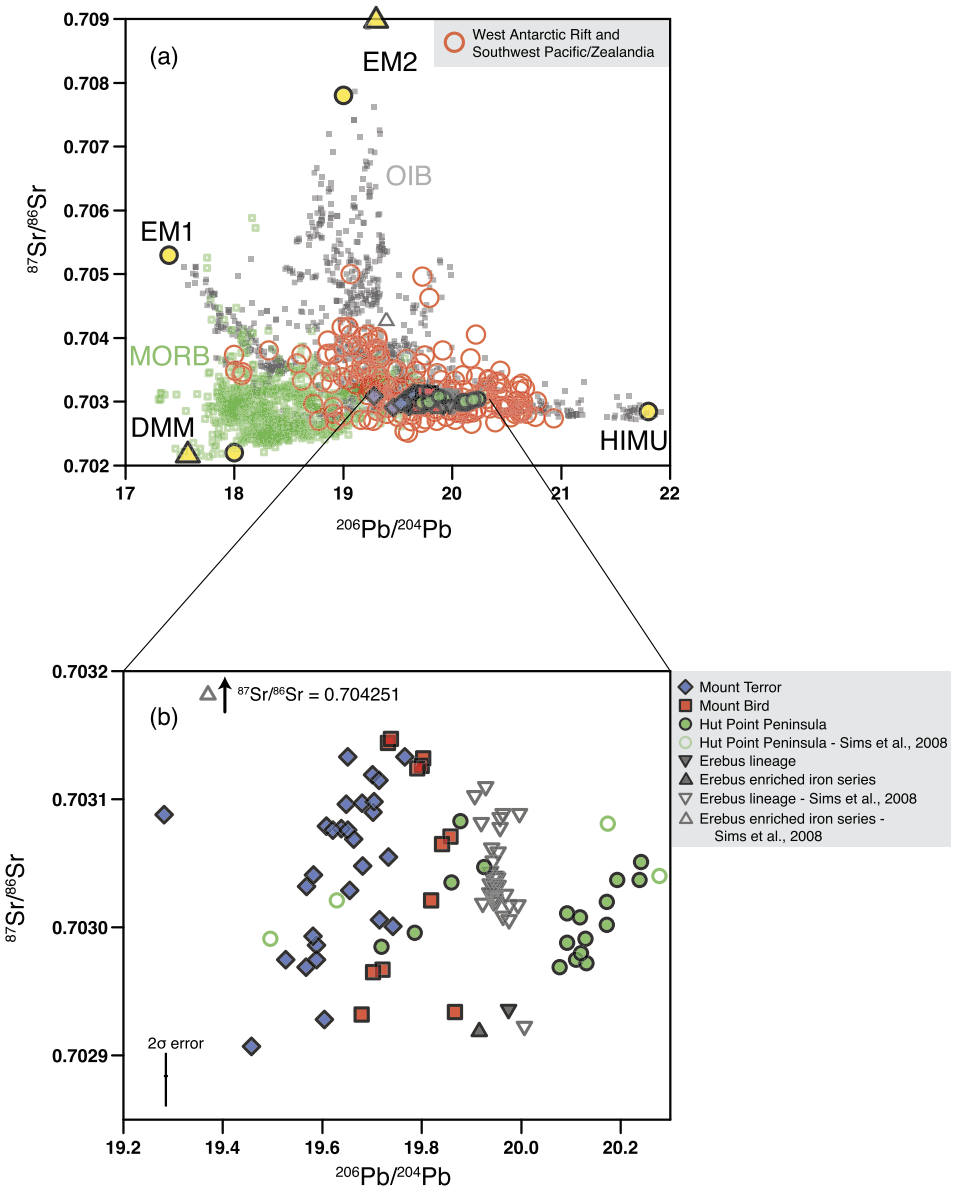

Fig. 5. $^{206}Pb/^{204}Pb$ versus $^{87}Sr/^{86}Sr$ showing the similarity of Ross Island lavas and tephras to those from the West Antarctic Rift and the greater southwest Pacific. (a) Ross Island volcanics in a global context (data from Sun and Hanson, 1975; Hart, 1988 (Balleny); Hart et al., 1995, 1997; Rocholl et al., 1995; Hoernle et al., 2006, 2010 [Hikurangi]; Panter et al., 2000, 2006; Timm et al., 2010; see also Finn et al., 2005). Mantle end-members are shown with yellow symbols; depleted MORB mantle (DMM) from Hart et al. (1992; circle) and Workman and Hart (2005; triangle); HIMU and enriched mantle 1 (EM1) from Hart et al. (1992); enriched mantle 2 (EM2) from Hart et al. (1992; circle) and Workman et al. (2004; triangle). Ross Island lavas and tephras are on a mixing line between the DMM and HIMU mantle end-members with a small possible contribution from an EM component. (b) Close-up of (a) showing Ross Island samples in detail. Error bars shown are 2σ external precision based on replicate measurements of standards (see Supplements A and D).

1997), are not observed in Mt. Bird rocks. Thus, if pelagic sediments are indeed at the origin of the isotopic differences at Mt. Bird compared to the rest of Ross Island, Hf isotopes are more sensitive than trace element proxies at identifying them.

Most Mt. Bird samples also have high $^{208}Pb/^{204}Pb$ for a given $^{206}Pb/^{204}Pb$ when compared to the rest of the Ross Island suite (Fig. 4c), indicating that the Mt. Bird samples incorporated source material with a different long-term U/Th ratio than the other Ross Island rocks. This overall slight divergence of Mt. Bird lavas and tephras from the main Ross Island trend suggests that the majority of Mt. Bird samples have incorporated a source component, or components, distinct from the rest of Ross Island.

Ross Island lavas and tephras primarily plot between the DMM and HIMU mantle end-members (Figs. 4, 5, 7, 8), suggesting they derive from partial melting of mantle peridotite containing these two components. A small but significant variability within the Ross Island volcanics, which creates a slight deviation from a simple two-component mixing relationship between DMM and HIMU, is consistent with the admixing of small amounts of an enriched mantle (EM) type of component.

Finally, we note that the isotopic compositions of four mineral separates demonstrate that they are co-genetic with their host lavas and tephras, lending additional credence to the notion that the isotope compositions of the whole-rock samples are good indicators of source composition (Fig. 4).

5.2. Sources and processes responsible for Ross Island magmatism

5.2.1. Rifting as a cause of Ross Island volcanism

Ross Island is located within a rift setting, and studies such as those of Rocchi et al. (2002, 2003) contend that magmatic activity in the West Antarctic Rift is closely linked in space and time to

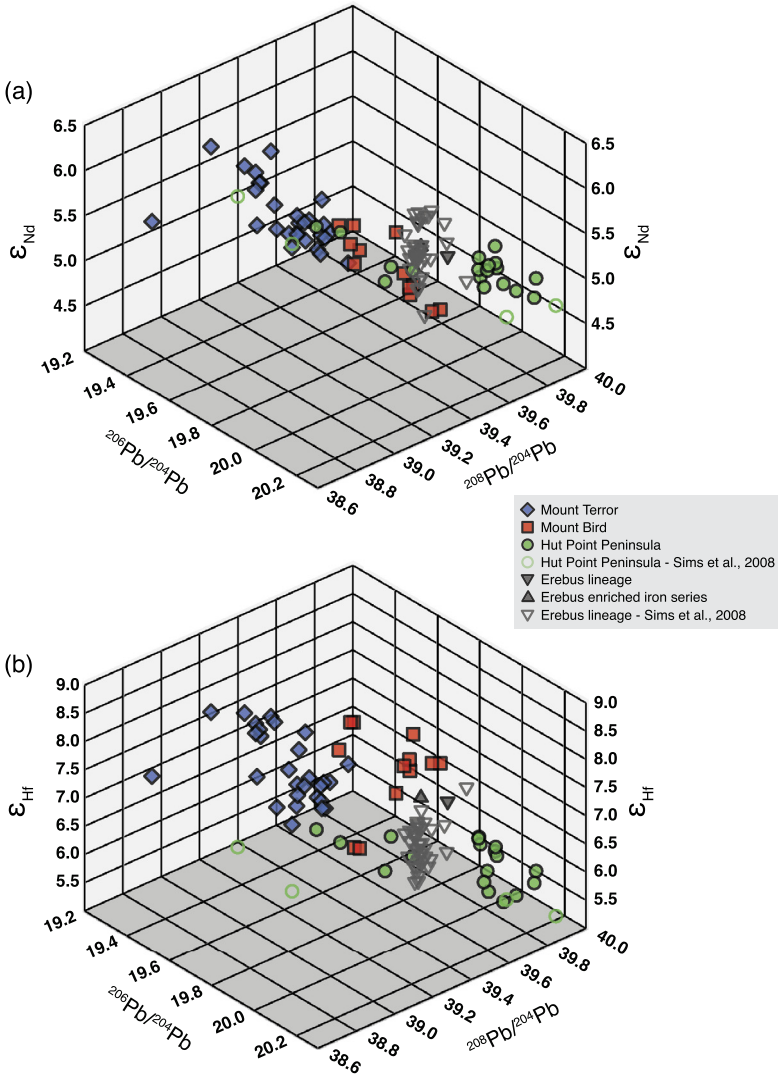

Fig. 6. Three-dimensional plots of ε_{Nd} (a) and ε_{Hf} (b) versus $^{206}Pb/^{204}Pb$ and $^{208}Pb/^{204}Pb$ showing the greater variability of the peripheral volcanic centers on Ross Island compared to Erebus volcano and the general clustering within each volcanic center. Mt. Terror lavas and tephras have the highest ε_{Nd} and ε_{Hf} and least radiogenic Pb isotope compositions, whereas Hut Point lavas and tephras have the most radiogenic Pb. For Mt. Bird, divergent trends emerge in Nd–Hf–Pb isotope space (see also Fig. 4), indicating that Mt. Bird tapped a slightly different mantle component. See Fig. 4 for error bars.

fault systems and is the result of decompression melting unrelated to mantle plumes. However, Sleep (2006) argued against a correlation between magmatism and rift tectonics in the West Antarctic Rift, noting that extension in Marie Byrd Land and Victoria Land had largely ceased before intraplate magmatism began in these regions. Present magmatic and recent eruptive activity (Lough et al., 2013) exists in Marie Byrd Land despite very low levels of ongoing rift extension (Bevis et al., 2009). Thus, we conclude that the large volume of magmatism expressed at Ross Island is not due to rift-associated extensional melting.

5.2.2. Ross Island's HIMU isotopic signature: a deep mantle plume or metasomatically enriched subcontinental lithosphere?

Cenozoic, dominantly alkaline volcanism in West Antarctica is widespread and a HIMU-like signature is ubiquitous in the Antarctic and southwest Pacific region, often referred to as Zealandia (Figs. 5 and 7). Ross Island is part of this volcanic province and is noteworthy because of its prolific and focused magmatism since ~4 Ma (~4500 km^3; Esser et al., 2004), pointing to a local thermal anomaly. The isotope compositions of regional volcanic rocks such as the Ferrar Group (~177 Ma; Fleming et al., 1995) and the distant minettes from East Antarctica (~455 Ma; Hoch et al., 2001) are more variable and enriched than at Ross Island, whereas at Ross Island all four long-lived isotope systems (Sr, Nd, Hf, and Pb) closely resemble HIMU (Figs. 4, 5, 7, 8). Three main hypotheses have been proposed to explain the HIMU signature at Ross Island. The first holds that Ross Island is the manifestation of a localized mantle thermal anomaly centered beneath Erebus volcano (Kyle et al., 1992; Storey et al., 1999). Sims et al. (2008) argued that Erebus lineage lavas (basanite through phonolite) and the restricted Sr, Nd, Hf, and Pb isotopic variations of Erebus volcano are best explained by melting of deep-seated mantle peridotite consisting of DMM and HIMU mantle components that mix to various extents (Figs. 4, 5, 7, 8). The other two hypotheses draw on the widespread nature of the HIMU-like signature in the Antarctic and southwest Pacific. Hart et al. (1997) studied HIMU-like lavas from Marie Byrd Land and proposed that a large deep-seated mantle plume with a HIMU signature impinged on the base of the Gondwana lithosphere prior to its breakup at ~85 Ma and noted the plausibility of its large plume head being associated with the Ferrar Large Igneous Province. In the model of Finn et al. (2005), the widespread regional HIMU-like signature is explained by melting of a metasomatized lithospheric source, with the presumed metasomatism occurring between 100 and 500 Ma in a sustained subduction

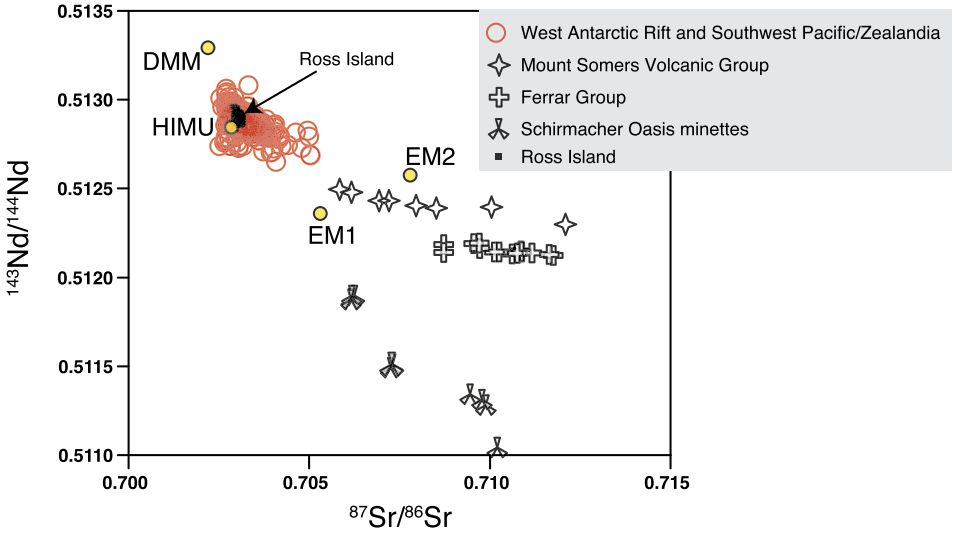

Fig. 7. $^{87}Sr/^{86}Sr$ versus $^{143}Nd/^{144}Nd$ comparing Ross Island lavas and tephras to rocks from the greater Antarctic and southwest Pacific region, highlighting the highly enriched isotopic signature of the older Mount Somers Volcanic Group (data from Tappenden, 2003), the Ferrar Group (Fleming et al., 1995), and the Schirmacher Oasis minettes of East Antarctica (Hoch et al., 2001), which are likely influenced by subduction-related metasomatically altered lithosphere. West Antarctic and southwest Pacific/Zealandia data from Futa and Le Masurier (1983), Hart (1988; Balleny), Hart et al. (1995, 1997), Rocholl et al. (1995), Hoernle et al. (2006, 2010 [Hikurangi]), Panter et al. (2000, 2006), Rocchi et al. (2002), and Timm et al. (2010). Ross Island data include samples from this study and from Sims et al. (2008), excluding enriched iron series samples. The isotopic dissimilarity between the Ross Island volcanics and the older Zealandia and Antarctic volcanic samples indicates that the source of the Ross Island lavas is old (Archean to early Proterozoic) material upwelling from the deep mantle rather than subcontinental lithospheric mantle metasomatized by Paleozoic subduction. Also shown are the values for the mantle end-members (yellow symbols; see Fig. 4 caption for references).

regime. Slab detachment in the late Cretaceous caused a change in mantle flow followed by onset of magmatism in the region at ~55 Ma. The metasomatized lithospheric source was later sampled by small degrees of partial melting. Panter et al. (2006) discussed the origin of the HIMU-like signature found in basalts from the Antipodes, Campbell, and Chatham Islands and likewise advocated for a widespread subduction-related metasomatized lithosphere as their primary source. We argue below that our new geochemical and isotopic data and geophysical modeling collectively point to a focused plume origin for Ross Island magmatism.

5.2.2.1. Physiographic observations Kyle et al. (1992) were the first to propose the presence of a mantle plume beneath Ross Island and noted that a large volume of mantle must have melted to produce the basanites that in turn differentiated into the large volume of phonolites erupted at Erebus volcano. Additionally, they pointed out that the geometry of volcanic upwelling at Ross Island is indicative of a cylindrical upwelling, in which the active Erebus volcano resides at the center with the peripheral volcanoes Mt. Terror, Mt. Bird, and Hut Point Peninsula radially surrounding Erebus at roughly ~120° angles, a geometric arrangement predicted by the modeling of Burke and Dewey (1973). Finally, Kyle et al. (1992) pointed out that the physical and geochemical characteristics of the Mt. Discovery complex, its current location and age, and the motion of the Antarctic plate are consistent with Mt. Discovery and its peripheral volcanoes being a previous locus of magmatism that resulted from the Ross Island thermal anomaly.

Geochemical and fluid mechanical models (e.g., Watson and McKenzie, 1991; Ribe and Christensen, 1994; Sims et al., 1999) suggest that mantle plumes have a clearly defined upwelling structure, which includes higher levels of entrainment on the cooler edges of plumes than at the center (Hauri et al., 1994). The overall greater variability in Sr, Nd, Hf, and Pb isotope compositions at the peripheral volcanic centers compared to Erebus volcano point to increased extents of mixing with surrounding heterogeneous lithosphere and/or asthenosphere at the periphery of Ross Island, consistent with the plume models of Hauri et al. (1994), which, as mentioned above, predict increased incorporation of ambient asthenosphere on the fringes of plumes (Figs. 4–6).

5.2.2.2. Geochemical observations A first-order observation is that Ross Island volcanics do not exhibit the same anomalous major element chemistry attributed to melting of a metasomatically altered source that is seen in unusual alkaline lavas such as lamprophyres and minettes (e.g., the minettes of the Schirmacher Oasis in East Antarctica; Hoch et al., 2001). Instead, the Ross Island lavas and tephras are basanitic or differentiates of parental basanites (e.g., phonolites) which have long been interpreted to represent small-degree partial melts of mantle peridotite (Green et al., 1967; Green, 1973). Further, depletion in heavy REE compared to middle REE in Ross Island lavas and tephras (mean $Dy_N/Yb_N \cong 1.4$; Fig. 3) and the observation that $(^{230}Th/^{238}U) > 1$ in Erebus lineage lavas require melting in the presence of residual garnet (Sun and Hanson, 1975; Sims and Hart, 2006; Sims et al., 2013). These observations imply that the Ross Island lavas and tephras were derived from a relatively deep source, below the garnet-spinel transition zone (i.e., below ~80 km depth). The seismologically estimated thickness of the lithosphere beneath West Antarctica is ~70–100 km (Heeszel et al., 2016; Lloyd et al., 2015). As such, the simplest interpretation of the Ross Island magmas is that they were derived by low-degree partial melting of garnet peridotite in the mantle asthenosphere.

From an isotopic viewpoint, the long-lived radiogenic isotope compositions of the Ross Island lavas and tephras are similar to the St. Helena HIMU mantle source (interpreted to be a deep mantle plume located in the mid-Atlantic) and do not resemble what would be expected from a metasomatically enriched subcontinental lithospheric source (Figs. 4, 5, 7, 8). Lavas interpreted to be lithospheric melts usually have more enriched isotopic signatures (i.e., lower ε_{Nd} and ε_{Hf}) than those found at Ross Island (e.g., Daley and DePaolo, 1992; Leat et al., 2005) because metasomatic enrichment will decrease Sm/Nd and Lu/Hf which as a consequence will grow in less radiogenic Nd and Hf over time leading to lower values of ε_{Nd} and ε_{Hf} (Reid et al., 2012). In this regard, we note that the older Antarctic samples, such as the minettes of the Schirmacher Oasis (~455 Ma; Hoch et al., 2001) and the Ferrar Group (~177 Ma; Fleming et al., 1995), show much more enriched and variable isotopic signatures (Figs. 7 and 8), consistent with melting of metasomatized lithosphere during Paleozoic subduction.

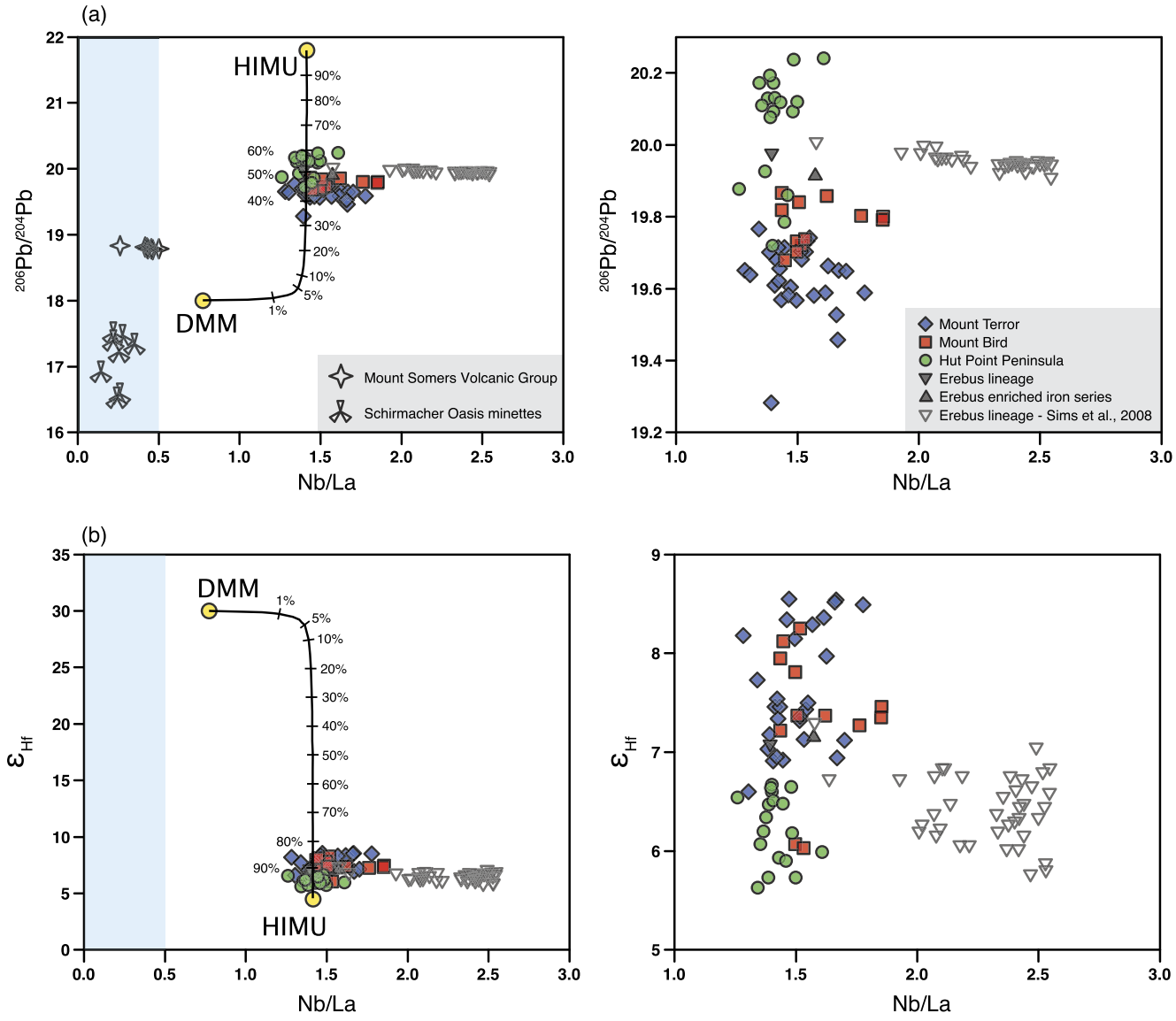

Fig. 8. Nb/La versus (a) $^{206}Pb/^{204}Pb$ and (b) ε_{Hf}, showing the difference between Ross Island volcanics and the Mount Somers Volcanic Group (MSVG; Tappenden, 2003) and the Schirmacher Oasis minettes (Hoch et al., 2001), and the position of Ross Island lavas and tephras on a mixing line between the HIMU and DMM mantle end-members. Left-hand side panels show Ross Island lavas and tephras in a global context. Also shown is St. Helena (yellow HIMU circle; Willbold and Stracke, 2006), which represents the HIMU mantle end-member, and Depleted MORB Mantle (yellow DMM circle; Workman and Hart, 2005) and the mixing compositions, with marked increments, between these two sources. The blue shaded region (Nb/La < 0.5) represents Nb/La ratios that reflect arc-related processes (Gill, 1981). Right-hand side panels are close-ups showing the Ross Island samples in detail. Timm et al. (2010) use the MSVG as a possible composition for Zealandia lithosphere enriched by subduction, and therefore its dissimilarity to Ross Island volcanics underlines the lack of influence from metasomatized subcontinental lithospheric mantle at Ross Island.

The quintessential aspect of the HIMU isotopic end-member is its radiogenic Pb isotope compositions, which reflect long-term enrichment of U and Th relative to Pb. While it is conceivable that a metasomatic enrichment of U, if strong enough, could lead relatively quickly (i.e., within <500 m.y.) to HIMU $^{206}Pb/^{204}Pb$ isotopic signatures because of the relatively short timescale of ^{238}U decay ($t_{1/2} = 4.5 \times 10^9$ yr), $^{207}Pb/^{204}Pb$ would not be significantly influenced in the last 500 m.y. because of Earth's current low abundance of ^{235}U, which has mostly decayed away. Preferential enrichment of Th relative to Pb likewise could lead to HIMU $^{208}Pb/^{204}Pb$ isotopic signatures, but on much longer timescales than the 500 m.y. in question here (^{232}Th $t_{1/2} = 1.4 \times 10^{10}$ yr). Similarly, it would take far longer for a metasomatic event to also affect the Sm–Nd and Lu–Hf isotope systems because of the significantly longer half-lives of ^{147}Sm (parent of ^{143}Nd; $t_{1/2} = 1.06 \times 10^{11}$ yr) and ^{176}Lu (parent of ^{176}Hf; $t_{1/2} = 3.71 \times 10^{10}$ yr) which are orders of magnitude longer than the half-lives of ^{238}U and ^{232}Th. Given these long half-lives, the relatively short time window since the alleged metasomatism (<500 m.y.), and the fact that all four long-lived isotope systems (Sr, Nd, Hf, and Pb) are similar to the St. Helena HIMU end-member, it is improbable that the HIMU characteristics of Ross Island represent melting of a relatively young (<500 m.y.) metasomatically altered lithosphere. Rather, the HIMU mantle end-member is consistent with an ancient (Archean to early Proterozoic) recycled source component thought to have become isolated in the lower mantle (Hanyu et al., 2011; Weiss et al., 2016), thereby allowing enough time for the characteristic HIMU isotopic signature to grow in for all isotopic systems over billions of years. We therefore argue that the Ross Island lavas contain a deep-seated, long-lived component that was brought to the surface by deep mantle upwelling.

Furthermore, the U–Th systematics of Erebus volcano are not consistent with arc-related metasomatic signatures. Arc-related metasomatism likely would enrich U over Th (e.g., Reubi et al., 2014,

and references therein) resulting in high $^{238}U/^{232}Th$ and high $^{230}Th/^{232}Th$ due to the decay of ^{238}U to ^{230}Th (over ~500 k.y.). Erebus samples have relatively low $^{230}Th/^{232}Th$ compared to global MORB and OIB compilations (Sims and Hart, 2006; Sims et al., 2013) and show $^{238}U/^{232}Th$ similar to the HIMU end-member (Sims and Hart, 2006), indicating that the parental basanites were not derived from a source that had been enriched in U relative to Th as would be expected from arc-related metasomatism.

Moreover, the trace element characteristics of the Ross Island volcanics also are not consistent with their derivation from a metasomatized lithospheric source altered by subduction processes. For example, in subduction regimes, the subcontinental lithosphere is expected to be depleted in high field strength elements (HFSE; e.g., Nb) relative to other incompatible elements because HFSE are retained in downgoing slabs (Kelemen et al., 1993); at the same time, fluid mobile elements such as La will be enriched. As such, ratios like Nb/La are important discriminants. In arcs Nb/La is universally <0.5 (Gill, 1981). The Ross Island lavas and tephras that we have analyzed (this study and Sims et al., 2008) all have Nb/La ratios in excess of 1.25, implying little involvement of a subduction metasomatized lithospheric component (Figs. 3 and 8). In a study of Zealandia volcanism, Timm et al. (2010) used New Zealand's Mount Somers Volcanic Group as an end-member composition for Zealandia magmas generated from subduction-related metasomatically altered lithosphere. In stark contrast to the Ross Island samples, the Mount Somers Volcanic Group samples (Tappenden, 2003) and the Schirmacher Oasis minettes from East Antarctica (Hoch et al., 2001) all have Nb/La <0.5, suggesting they are either sourced from or have assimilated significant amounts of metasomatized lithospheric mantle (Fig. 8). We thus interpret the Nb/La > 0.5 of the Ross Island volcanics as a contraindication of their being derived by melting or assimilation of a lithospheric source altered by subduction processes. Finally, we note that the Ross Island samples from Mt. Bird, Mt. Terror, and Hut Point Peninsula lie on a mixing curve between DMM and HIMU (Fig. 8), consistent with trends also observed among Sr, Nd, Hf, and Pb isotopes. The high Nb/La trend seen in the Erebus lavas relative to lavas from its peripheral volcanoes reflects variable extents of fractionation of apatite, a phase which is present in Erebus lavas at ~0.5% modal abundance (Kyle, 1981; Kyle et al., 1992).

In further support of a deep HIMU plume hypothesis, we note that eleven olivines from hyaloclastites from the DVDP core at Ross Island have $^{3}He/^{4}He$ (R/R_a values with an error-weighted mean of 6.91; Parmelee et al., 2015) similar to St. Helena (R/R_a of 5.24 to 5.97; Hanyu et al., 2014). While high $^{3}He/^{4}He$ is thought to be indicative of undegassed primitive mantle due to the primordial nature of ^{3}He, lavas derived from the HIMU mantle end-member at plumes such as St. Helena typically have low $^{3}He/^{4}He$, which is attributed to the presence of radiogenic ^{4}He in the recycled materials that form the deep HIMU mantle reservoir (Graham et al., 1992; Parai et al., 2009; Hanyu et al., 2014).

5.2.2.3. Geophysical observations Regional seismic data collected across Antarctica reveal a prominent low-velocity zone in the upper mantle beneath Ross Island in particular (Watson et al., 2006; Zhao, 2007; Gupta et al., 2009; Heeszel et al., 2016) and the WARS in general (Ritzwoller et al., 2001), implying elevated temperatures. The regional tomographic body wave inversion of Hansen et al. (2014) highlights extensive low velocities within the upper ~200–300 km of the mantle but has insufficient resolution to image low velocities at greater depths. However, global tomographic modeling using finite-frequency kernels (Montelli et al., 2006) and full-waveform inversion (Bozdağ et al., 2016; Fig. 9; see French and Romanowicz, 2015), although at much broader resolution, indicate a sub-mantle transition zone low shear wave seismic velocity anomaly that extends to ~1200 km depth beneath Ross Island, with linked features that extend eastward beneath the WARS and below the Marie Byrd Land volcanic province. Low-velocity sub-transition zone structure is also corroborated in the independent models SGLOBE-rani (Chang et al., 2015) and GyPSuM (Simmons et al., 2010), and in the composite model SMEAN2 (Becker and Boschi, 2002; Simmons et al., 2010; Ritsema et al., 2011; Auer et al., 2014) (Supplement F). These global images, which benefit from vastly expanded recent seismographic data recorded in Antarctica (e.g., Anthony et al., 2015), are consistent with the hypothesis that a deep mantle thermal structure is driving the melting that ultimately produced the observed HIMU signature.

5.3. Evolution of the magma source of Antarctic volcanics

Noting the widespread regional HIMU-like signature of Ross Island and greater West Antarctica and the finding that plate reconstruction models indicate prolonged subduction in the Paleozoic–Mesozoic (~500–100 Ma) along the Pacific margin of Gondwana (Finn et al., 2005; Seton et al., 2012), Finn et al. (2005) suggested that "common geological, geochemical, and geophysical characteristics of continental fragments of East Gondwana and adjacent oceanic lithosphere define a long-lived, low-volume, diffuse alkaline magmatic province (which the authors termed DAMP) encompassing the easternmost part of the Indo-Australian Plate, West Antarctica, and the southwest portion of the Pacific Plate". As such they suggested that the ubiquitous HIMU-like signature seen in the lavas represents melting of a metasomatized lithospheric source, the product of long-lived subduction along Gondwana's Pacific margin.

However, as discussed in detail above (section 5.2.2.2; Figs. 7 and 8), an important distinction exists between the trace element and isotopic characteristics of the older Zealandia and Antarctic volcanic samples and those of Ross Island lavas and tephras. Given these marked geochemical differences and the recent geophysical observation that an active sub-transition zone is upwelling below Ross Island and the WARS (Fig. 9), we argue that, while ancient subduction processes occurring along the Pacific margin of Gondwana undoubtedly influenced the lithosphere beneath the southwest Pacific and Antarctica and may have produced radiogenic Pb isotope compositions akin to HIMU, this metasomatized material is no longer the source of lavas being erupted at Ross Island. Rather, the Ross Island volcanics are best explained as deriving from an asthenospheric source that is a mixture of DMM and HIMU, as attested to by all four long-lived radiogenic isotopic systems (Sr, Nd, Hf, and Pb), not just the Pb isotopes alone. We hence conclude that Ross Island lavas and tephras represent melting of a deep-seated, long-lived component, such as the HIMU mantle end-member thought to be ancient (Archean to early Proterozoic) recycled oceanic crust isolated in the lower mantle for billions of years (Hanyu et al., 2011; Weiss et al., 2016), thereby allowing the characteristic HIMU isotopic signature to grow in over time in all four isotopic systems (Sr, Nd, Hf, and Pb), even the longest-lived among them. We further contend that, by now, large-scale mantle upwelling has eroded away the metasomatic signature relict from the Paleozoic to Mesozoic subduction that took place along the margins of Gondwana. It is not surprising that the relict metasomatic signature has been completely removed beneath Ross Island given the large amount of magma that has been produced under this island (4520 km^3 of erupted material over the last four million years; Esser et al., 2004) and the slow motion of the Antarctic lithosphere (14 mm/yr in a south-southeasterly direction using the hotspot reference frame HS2-NUVEL 1A; Argus and Gordon, 1991) causing the lithosphere to be left in place for long enough to become thoroughly eroded.

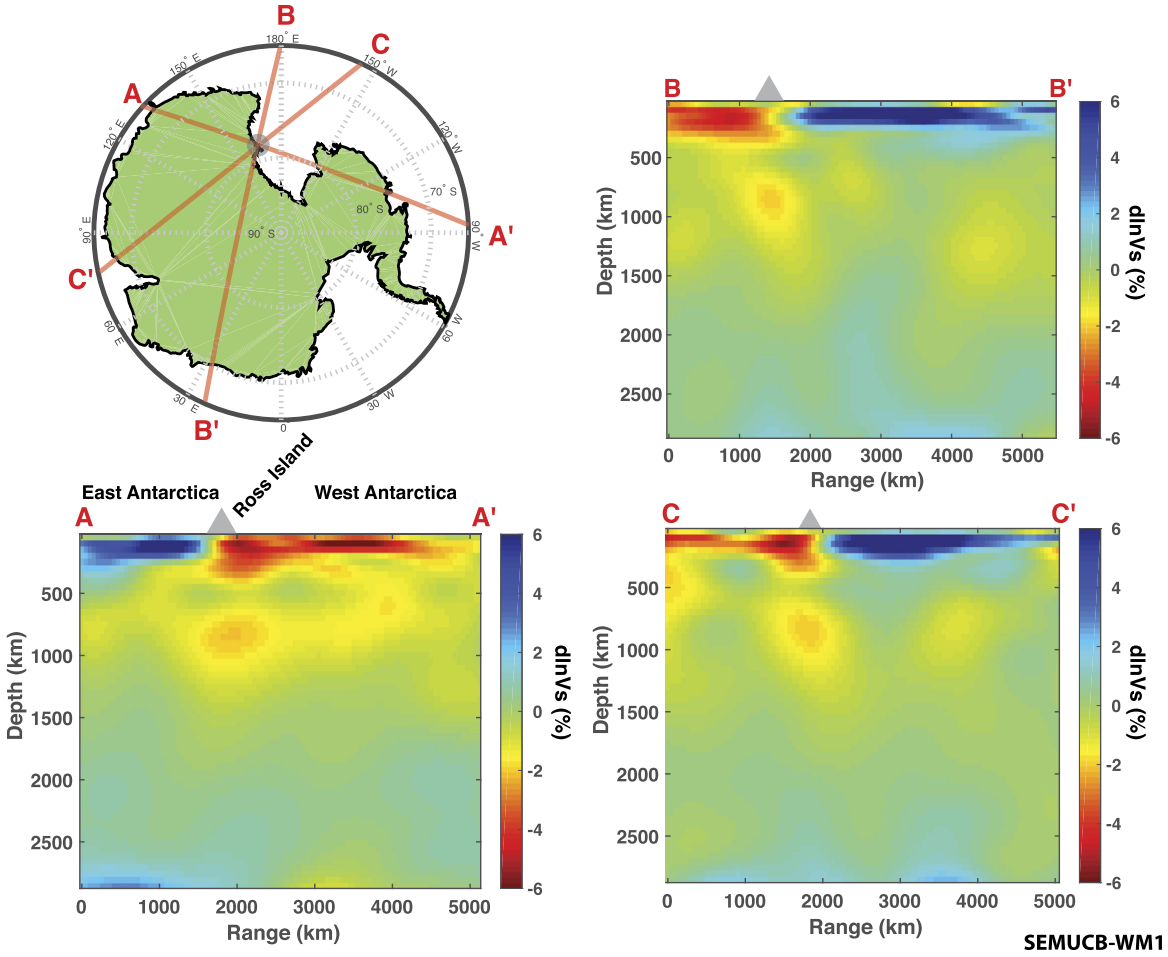

Fig. 9. Seismic tomography transects through Ross Island for three azimuths (upper left) displaying the isotropically averaged seismic shear wave velocity anomaly from the crust to the core–mantle boundary in global velocity model SEMUCB-WM1 (French and Romanowicz, 2015). This and other recent tomography models of the region indicate a low seismic shear wave velocity anomaly that extends below the mantle transition zone to near 1200 km depth beneath Ross Island, with linked features that extend eastward beneath the West Antarctic Rift System into the volcanic province of Marie Byrd Land. The color scale indicates the relative perturbation of shear wave velocity compared to the corresponding model 1-dimensional depth average. SEMUCB-WM1 was calculated using full-waveform inversion of a large data set of long period body (>32 s) and surface (>60 s) wave global seismograms. Comparable lower mantle features are also present in the full waveform inversion model GLAD-M15 of Bozdağ et al. (2016) and in other global models (see Supplement F).

6. Conclusions

We provide an extensive geochemical and isotopic data set for Mt. Terror, Mt. Bird, and Hut Point Peninsula to complement an equally extensive and similar existing data set for Erebus (Kelly et al., 2008; Sims et al., 2008). Using geophysical, geochemical, and isotopic constraints and examining all four volcanic centers at Ross Island together, this integrated, multi-disciplinary study sheds new light on the driving forces of alkaline volcanism beneath Ross Island and the nature and evolution of its HIMU source. Three new holistic perspectives on this unique and important volcanic complex have emerged from the present study.

First, although the Sr, Nd, Hf, and Pb isotope compositions of all four volcanic centers (Erebus, Mt. Terror, Mt. Bird, and Hut Point Peninsula) can be broadly modeled as a mixture of HIMU and DMM, there is significant variability between these centers and a general clustering of isotope compositions among them. This inter-volcano isotopic variability implies a length scale of mantle heterogeneity beneath Ross Island comparable to or smaller than that of inter-volcano distances (i.e., <50 km). Further, Mt. Bird lavas and tephras have isotope compositions distinct from the other three volcanoes, pointing to a separate source component, possibly deep-sea pelagic sediments, tapped only by Mt. Bird.

Second, several lines of evidence suggest that Ross Island is the surface manifestation of a deep upwelling mantle plume: (1) The three peripheral volcanic centers radially surround the active Erebus volcano at 120° angles, consistent with the plume structure modeling of Burke and Dewey (1973); (2) the greater overall Sr, Nd, Hf, and Pb isotopic variability of Mt. Terror, Mt. Bird, and Hut Point Peninsula lavas and tephras compared to Erebus volcano samples suggests increased asthenospheric and/or lithospheric entrainment and mixing at the periphery of Ross Island consistent with fluid dynamical models of plume upwelling (Hauri et al., 1994); and (3) independent seismic tomography models resolve a low shear wave velocity zone that extends to ∼1200 km beneath Ross Island and into greater West Antarctica, suggesting that the mantle melting responsible for the HIMU signature has a deep-seated origin.

Third, an important distinction is observed between both the geochemical and isotopic characteristics of the older Zealandia and Antarctic volcanic samples and the Ross Island lavas and tephras. Namely: (1) All four isotope systems (Sr, Nd, Hf, and Pb), not just Pb isotopes alone, show compositions similar to the HIMU mantle end-member (e.g., as represented by St. Helena); and (2) trace element signatures of the Ross Island lavas such as Nb/La are inconsistent with a metasomatized mantle influence, unlike

the Zealandia Mount Somers Volcanic Group and older Antarctic samples such as the Ferrar group and the minettes from East Antarctica.

We therefore posit that the source of the Ross Island lavas is old (Archean to early Proterozoic) material upwelling from the deep mantle rather than subcontinental lithospheric mantle that was metasomatized by Paleozoic subduction. Thus, while the process of Paleozoic subduction along Gondwana likely strongly affected the lithosphere beneath the southwest Pacific and Antarctica, we argue that this metasomatized material has been thermally eroded away beneath Ross Island and is not the source of lavas currently being erupted there.

Acknowledgements

This work was funded by National Science Foundation awards OPP-ANT-1141167 (KWWS), NSF-OPP ANT-1644013 (KWWS), EAR-0960270 (KWWS), ANT-1141534 (PRK) and OPP-ANT-1419268 (RCA). JBT acknowledges financial support from the French Agence Nationale de la Recherche through grant ANR-10-BLAN-0603 (M&Ms — Mantle Melting — Measurements, Models, Mechanisms). Geospatial support for this work was provided by the Polar Geospatial Center under NSF OPP awards 1043681 & 1559691. Additional funding was provided to EHP by the Dick and Lynne Cheney Fellowship for Excellence in Study Abroad, the University of Wyoming Department of Geology and Geophysics, the Roy J. Schlemon Center for Quaternary Studies, and a Goldschmidt Student Travel Grant. Global model sections were facilitated by the IRIS Earth Modeling Collaboration (Trabant et al., 2012). Code and data for the SEMUCB-WM1 model was provided by Barbara Romanowicz and colleagues at the University of California, Berkeley. NSF-directed Antarctic support personnel made fieldwork in Antarctica smooth and efficient. EHP is grateful to ENS Lyon for its hospitality and to Philippe Telouk and Francis Albarède for help and guidance. We further thank Susan Swapp, Tyler Brown, Sean Scott, and Evan Soderberg for assistance with sample preparation and analyses. We appreciate constructive discussions with Sean Scott and Mark Reagan. Comments by two anonymous reviewers and editor Tamsin Mather significantly improved the manuscript.

Appendix A. Supplementary material

Supplementary material related to this article can be found online at https://doi.org/10.1016/j.epsl.2018.05.049.

References

Anthony, R.E., Aster, R.C., Wiens, D., Nyblade, A., Anandakrishnan, S., Huerta, A.D., Winberry, J.P., Wilson, T., Rowe, C., 2015. The seismic noise environment of Antarctica. Seismol. Res. Lett. 86, 89–100. https://doi.org/10.1785/0220140109.

Argus, D.F., Gordon, R.G., 1991. No-net-rotation model of current plate velocities incorporating plate motion model NUVEL-1. Geophys. Res. Lett. 18, 2039–2042. https://doi.org/10.1029/91gl01532.

Armstrong, R.L., 1978. K–Ar dating: Late Cenozoic McMurdo Volcanic Group and dry valley glacial history, Victoria Land, Antarctica. N.Z. J. Geol. Geophys. 21, 685–698. https://doi.org/10.1080/00288306.1978.10425199.

Auer, L., Boschi, L., Becker, T.W., Nissen-Meyer, T., Giardini, D., 2014. Savani: a variable-resolution whole-mantle model of anisotropic shear-velocity variations based on multiple datasets. J. Geophys. Res. 119, 3006–3034. https://doi.org/10.1002/2013jb010773.

Bannister, S., Yu, J., Leitner, B., Kennett, B.L.N., 2003. Variations in crustal structure across the transition from West to East Antarctica, Southern Victoria Land. Geophys. J. Int. 155, 870–884. https://doi.org/10.1111/j.1365-246x.2003.02094.x.

Becker, T.W., Boschi, L., 2002. A comparison of tomographic and geodynamic mantle models. Geochem. Geophys. Geosyst. 3. https://doi.org/10.1029/2001gc000168.

Behrendt, J.C., 1999. Crustal and lithospheric structure of the west Antarctic Rift System from geophysical investigations — a review. Glob. Planet. Change 23, 25–44. https://doi.org/10.1016/s0921-8181(99)00049-1.

Bevis, M., Kendrick, E., Smalley, R., Dalziel, I., Caccamise, D., Sasgen, I., Helsen, M., Taylor, F.W., Zhou, H., Brown, A., Raleigh, D., Willis, M., Wilson, T., Konfal, S., 2009. Geodetic measurements of vertical crustal velocity in West Antarctica and the implications for ice mass balance. Geochem. Geophys. Geosyst. 10. https://doi.org/10.1029/2009gc002642.

Blichert-Toft, J., Frey, F.A., Albarède, F., 1999. Hf isotope evidence for pelagic sediments in the source of Hawaiian basalts. Science 285, 879–882. https://doi.org/10.1126/science.285.5429.879.

Bozdağ, E., Peter, D., Lefebvre, M., Komatitsch, D., Tromp, J., Hill, J., Podhorszki, N., Pugmire, D., 2016. Global adjoint tomography: first-generation model. Geophys. J. Int. 207, 1739–1766. https://doi.org/10.1093/gji/ggw356.

Burke, K., Dewey, J.F., 1973. Plume-generated triple junctions: key indicators in applying plate tectonics to old rocks. J. Geol. 81, 406–433.

Chang, S.-J., Ferreira, A.M.G., Ritsema, J., van Heijst, H.J., Woodhouse, J.H., 2015. Joint inversion for global isotropic and radially anisotropic mantle structure including crustal thickness perturbations. J. Geophys. Res. 120, 4278–4300. https://doi.org/10.1002/2014jb011824.

Chaput, J., Aster, R.C., Huerta, A.D., Sun, X., Lloyd, A., Wiens, D., Nyblade, A., Anandakrishan, S., Winberry, J.P., Wilson, T., 2014. The crustal thickness of West Antarctica. J. Geophys. Res. 119, 1–18. https://doi.org/10.1002/2013jb010642.

Cole, J.W., Kyle, P.R., Neall, V.E., 1971. Contribution to Quaternary geology of Cape Crozier, White Island and Hut Point Peninsula, McMurdo Sound region, Antarctica. N.Z. J. Geol. Geophys. 14, 528–546. https://doi.org/10.1080/00288306.1971.10421946.

Daley, E.E., DePaolo, D.J., 1992. Isotopic evidence for lithospheric thinning during extension: Southeastern Great Basin. Geology 20, 104–108. https://doi.org/10.1130/0091-7613(1992)020<0104:iefltd>2.3.co;2.

Esser, R.P., Kyle, P.R., McIntosh, W.C., 2004. $^{40}Ar/^{39}Ar$ dating of the eruptive history of Mount Erebus, Antarctica: volcano evolution. Bull. Volcanol. 66, 671–686. https://doi.org/10.1007/s00445-004-0354-x.

Finn, C.A., Müller, R.D., Panter, K.S., 2005. A Cenozoic diffuse alkaline magmatic province (DAMP) in the southwest Pacific without rift or plume origin. Geochem. Geophys. Geosyst. 6. https://doi.org/10.1029/2004gc000723.

Finotello, M., Nyblade, A., Julia, J., Wiens, D., Anandakrishnan, S., 2011. Crustal Vp–Vs ratios and thickness for Ross Island and the Transantarctic Mountain front, Antarctica. Geophys. J. Int. 185, 85–92. https://doi.org/10.1111/j.1365-246x.2011.04946.x.

Fleming, T.H., Foland, K.A., Elliot, D.H., 1995. Isotopic and chemical constraints on the crustal evolution and source signature of Ferrar magmas, north Victoria Land, Antarctica. Contrib. Mineral. Petrol. 121, 217–236.

French, S.W., Romanowicz, B., 2015. Broad plumes rooted at the base of the Earth's mantle beneath major hotspots. Nature 525, 95–99. https://doi.org/10.1038/nature14876.

Futa, K., Le Masurier, W.E., 1983. Nd and Sr isotopic studies on cenozoic mafic lavas from West Antarctica: another source for continental alkali basalts. Contrib. Mineral. Petrol. 83, 38–44.

Gill, J., 1981. Orogenic Andesites and Plate Tectonics. Springer-Verlag, Berlin.

Graham, D.W., Humphris, S.E., Jenkins, W.J., Kurz, M.D., 1992. Helium isotope geochemistry of some volcanic rocks from Saint Helena. Earth Planet. Sci. Lett. 110, 121–131. https://doi.org/10.1016/0012-821x(92)90043-u.

Green, D.H., 1973. Conditions of melting of basanite magma from garnet peridotite. Earth Planet. Sci. Lett. 17, 456–465.

Green, T.H., Green, D.H., Ringwood, A.E., 1967. The origin of high-alumina basalts and their relationships to quartz tholeiites and alkali basalts. Earth Planet. Sci. Lett. 2, 41–51.

Gupta, S., Zhao, D., Rai, S.S., 2009. Seismic imaging of the upper mantle under the Erebus hotspot in Antarctica. Gondwana Res. 16, 109–118. https://doi.org/10.1016/j.gr.2009.01.004.

Hansen, S.E., Graw, J.H., Kenyon, L.M., Nyblade, A.A., Wiens, D.A., Aster, R.C., Huerta, A.D., Anandakrishnan, S., Wilson, T., 2014. Imaging the Antarctic mantle using adaptively parameterized P-wave tomography: evidence for heterogeneous structure beneath West Antarctica. Earth Planet. Sci. Lett. 408, 66–78. https://doi.org/10.1016/j.epsl.2014.09.043.

Hanyu, T., Kawabata, H., Tatsumi, Y., Kimura, J., Hyodo, H., Sato, K., Miyazaki, T., Chang, Q., Hirahara, Y., Takahashi, T., Senda, R., Nakai, S., 2014. Isotope evolution in the HIMU reservoir beneath St. Helena: implications for the mantle recycling of U and Th. Geochim. Cosmochim. Acta 143, 232–252. https://doi.org/10.1016/j.gca.2014.03.016.

Hanyu, T., Tatsumi, Y., Senda, R., Miyazaki, T., Chang, Q., Hirahara, Y., Takahashi, T., Kawabata, H., Suzuki, K., Kimura, J., 2011. Geochemical characteristics and origin of the HIMU reservoir: a possible mantle plume source in the lower mantle. Geochem. Geophys. Geosyst. 12. https://doi.org/10.1029/2010gc003252.

Harpel, C.J., Kyle, P.R., Esser, R.P., McIntosh, W.C., Caldwell, D.A., 2004. $^{40}Ar/^{39}Ar$ dating of the eruptive history of Mount Erebus, Antarctica: summit flows, tephra, and caldera collapse. Bull. Volcanol. 66, 687–702. https://doi.org/10.1007/s00445-004-0354-x.

Hart, S.R., Blusztajn, J., LeMasurier, W., Rex, D., 1997. Hobbs Coast Cenozoic volcanism: implications for the West Antarctic rift system. Chem. Geol. 139, 223–248. https://doi.org/10.1016/s0009-2541(97)00037-5.

Hart, S.R., Blusztajn, J., Craddock, C., 1995. Cenozoic volcanism in Antarctica: Jones Mountains and Peter I Island. Geochim. Cosmochim. Acta 59, 3379–3388. https://doi.org/10.1016/0016-7037(95)00212-i.

Hart, S.R., Hauri, E.H., Oschmann, L.A., Whitehead, J.A., 1992. Mantle plumes and entrainment: isotopic evidence. Science 256, 517–520. https://doi.org/10.1126/science.256.5056.517.

Hart, S.R., 1988. Heterogeneous mantle domains: signatures, genesis and mixing chronologies. Earth Planet. Sci. Lett. 90, 273–296. https://doi.org/10.1016/0012-821x(88)90131-8.

Hauri, E.H., Whitehead, J.A., Hart, S.R., 1994. Fluid dynamic and geochemical aspects of entrainment in mantle plumes. J. Geophys. Res. 99, 24,275–24,300. https://doi.org/10.1029/94jb01257.

Heeszel, D.S., Wiens, D., Anandakrishnan, S., Aster, R.C., Dalziel, I.W.D., Huerta, A.D., Nyblade, A.A., Wilson, T.J., Winberry, J.P., 2016. Upper mantle structure of central and West Antarctica from array analysis of Rayleigh wave phase velocities. J. Geophys. Res., Solid Earth 121, 1758–1775. https://doi.org/10.1002/2015jb012616.

Hoch, M., Rehkämper, M., Tobschall, H.J., 2001. Sr, Nd, Pb and O isotopes of Minettes from Schirmacher Oasis, East Antarctica: a case of mantle metasomatism involving subducted continental material. J. Petrol. 42, 1387–1400. https://doi.org/10.1093/petrology/42.7.1387.

Hoernle, K., Hauff, F., van den Bogaard, P., Werner, R., Mortimer, N., Geldmacher, J., Garbe-Schönberg, D., Davy, B., 2010. Age and geochemistry of volcanic rocks from the Hikurangi and Manihiki oceanic Plateaus. Geochim. Cosmochim. Acta 74, 7196–7219. https://doi.org/10.1016/j.gca.2010.09.030.

Hoernle, K., White, J.D.L., van den Bogaard, P., Hauff, F., Coombs, D.S., Werner, R., Timm, C., Garbe-Schönberg, D., Reay, A., Cooper, A.R., 2006. Cenozoic intraplate volcanism on New Zealand: upwelling induced by lithospheric removal. Earth Planet. Sci. Lett. 248, 350–367. https://doi.org/10.1016/j.epsl.2006.06.001.

Iacovino, K., Oppenheimer, C., Scaillet, B., Kyle, P., 2016. Storage and evolution of mafic and intermediate alkaline magmas beneath Ross Island, Antarctica. J. Petrol. 57, 93–118. https://doi.org/10.1093/petrology/egv083.

Kelemen, P.B., Shimizu, N., Dunn, T., 1993. Relative depletion of niobium in some arc magmas and the continental crust: partitioning of K, Nb, La, and Ce during melt/rock reaction in the upper mantle. Earth Planet. Sci. Lett. 120, 111–134. https://doi.org/10.1016/0012-821x(93)90234-z.

Kelly, P.J., Kyle, P.R., Dunbar, N.W., Sims, K.W.W., 2008. Geochemistry and mineralogy of the phonolite lava lake, Erebus volcano, Antarctica: 1972–2004 and comparison with older lavas. J. Volcanol. Geotherm. Res. 177, 589–605. https://doi.org/10.1016/j.jvolgeores.2007.11.025.

Knox, H.A., Chaput, J.A., Aster, R.C., Kyle, P.R., 2018. Multiyear shallow conduit changes observed with lava lake eruption seismograms at Erebus volcano, Antarctica. J. Geophys. Res., Solid Earth 123 (4), 3178–3196. https://doi.org/10.1002/2017jb015045.

Kyle, P.R., 1981. Mineralogy and geochemistry of a basanite to phonolite sequence at Hut Point Peninsula, Antarctica, based on core from Dry Valley drilling Project Drillholes 1, 2 and 3. J. Petrol. 22, 451–500. https://doi.org/10.1093/petrology/22.4.451.

Kyle, P.R., 1990a. Erebus volcanic province. In: LeMasurier, W.E., Thomson, J. (Eds.), Volcanoes of the Antarctic Plate and Southern Oceans. In: Antarctic Research Series. American Geophysical Union, Washington DC, pp. 81–88.

Kyle, P.R., 1990b. McMurdo Volcanic Group—western Ross embayment: introduction. In: Le Masurier, W.E., Thomson, J. (Eds.), Volcanoes of the Antarctic Plate and Southern Oceans. In: Antarctic Research Series. American Geophysical Union, Washington DC, pp. 18–25.

Kyle, P.R., Moore, J.A., Thirlwall, M.F., 1992. Petrologic evolution of anorthoclase phonolite lavas at Mount Erebus, Ross Island, Antarctica. J. Petrol. 33, 849–875. https://doi.org/10.1093/petrology/33.4.849.

Leat, P.T., Dean, A.A., Millar, I.L., Kelley, S.P., Vaughan, A.P.M., Riley, T.R., 2005. Lithospheric mantle domains beneath Antarctica. Geol. Soc. (Lond.) Spec. Publ. 246, 359–380. https://doi.org/10.1144/gsl.sp.2005.246.01.15.

Li, C., van der Hilst, R.D., Engdahl, E.R., Burdick, S., 2008. A new global model for P wave speed variations in Earth's mantle. Geochem. Geophys. Geosyst. 9. https://doi.org/10.1029/2007gc001806.

Lloyd, A., Wiens, D., Nyblade, A., Anandakrishan, S., Aster, R., Huerta, A., Wilson, A.H., Dalziel, I., Shore, P.J., Zhao, D., 2015. A seismic transect across West Antarctica: evidence for mantle thermal anomalies beneath the Bentley Subglacial Trench and the Marie Byrd Land Dome. J. Geophys. Res. 120, 8439–8460. https://doi.org/10.1002/2015jb012455.

Lough, A.C., Wiens, D.A., Barcheck, C.G., Anandakrishnan, S., Aster, R.C., Blankenship, D.D., Huerta, A.D., Nyblade, A., Young, D.A., Wilson, T.J., 2013. Seismic detection of an active subglacial magmatic complex in Marie Byrd Land, Antarctica. Nat. Geosci. 6 (12), 1031–1035. https://doi.org/10.1038/ngeo1992.

McDonough, W.F., Sun, S.S., 1995. The composition of the Earth. Chem. Geol. 120, 223–253. https://doi.org/10.1016/0009-2541(94)00140-4.

Montelli, R., Nolet, G., Dahlen, F.A., Masters, G., 2006. A catalogue of deep mantle plumes: new results from finite frequency tomography. Geochem. Geophys. Geosyst. 7. https://doi.org/10.1029/2006gc001248.

Nolet, G., Karato, S.-I., Montelli, R., 2006. Plume fluxes from seismic tomography. Earth Planet. Sci. Lett. 248, 685–699. https://doi.org/10.1016/j.epsl.2006.06.011.

Panter, K.S., Blusztajn, J., Hart, S.R., Kyle, P.R., Esser, R., McIntosh, W.C., 2006. The origin of HIMU in the SW Pacific: evidence from intraplate volcanism in Southern New Zealand and subantarctic islands. J. Petrol. 47, 1673–1704. https://doi.org/10.1093/petrology/egl024.

Panter, K.S., Hart, S.R., Kyle, P., Blusztajn, J., Wilch, T., 2000. Geochemistry of Late Cenozoic basalts from the Crary Mountains: characterization of mantle sources in Marie Byrd Land, Antarctica. Chem. Geol. 165, 215–241. https://doi.org/10.1016/s0009-2541(99)00171-0.

Parai, R., Mukhopadhyay, S., Lassiter, J.C., 2009. New constraints on the HIMU mantle from neon and helium isotopic compositions of basalts from the Cook–Austral Islands. Earth Planet. Sci. Lett. 277, 253–261. https://doi.org/10.1016/j.epsl.2008.10.014.

Parmelee, D.E.F., Kyle, P.R., Kurz, M.D., Marrero, S.M., Phillips, F.M., 2015. A new Holocene eruptive history of Erebus volcano, Antarctica using cosmogenic ^{3}He and ^{36}Cl exposure ages. Quat. Geochronol. 30, 114–131. https://doi.org/10.1016/j.quageo.2015.09.001.

Rasmussen, D.J., Kyle, P.R., Wallace, P.J., Sims, K.W.W., Gaetani, G.A., Phillips, E.H., 2017. Understanding degassing and transport of CO_2-rich alkalic magmas at Ross Island, Antarctica using olivine-hosted melt inclusions. J. Petrol. 58, 841–861. https://doi.org/10.1093/petrology/egx036.

Reid, M.R., Bouchet, R.A., Blichert-Toft, J., Levander, A., Liu, K., Miller, M.S., Ramos, F.C., 2012. Melting under the Colorado Plateau, USA. Geology 40, 387–390. https://doi.org/10.1130/g32619.1.

Reubi, O., Sims, K.W.W., Bourdon, B., 2014. ^{238}U–^{230}Th equilibrium in arc magmas and implications for the time scales of mantle metasomatism. Earth Planet. Sci. Lett. 391, 146–158. https://doi.org/10.1016/j.epsl.2014.01.054.

Ribe, N.M., Christensen, U.R., 1994. Three-dimensional modeling of plume–lithosphere interaction. J. Geophys. Res. 99, 669–682. https://doi.org/10.1029/93jb02386.

Ritsema, J., van Heijst, H.J., Deuss, A., Woodhouse, J.H., 2011. S40RTS: a degree-40 shear-velocity model for the mantle from new Rayleigh wave dispersion, teleseismic traveltimes, and normal-mode splitting function measurements. Geophys. J. Int. 184. https://doi.org/10.1111/j.1365-246x.2010.04884.x.

Ritzwoller, M.H., Shapiro, N.M., Levshin, A.L., Leahy, G.M., 2001. Crustal and upper mantle structure beneath Antarctica and surrounding oceans. J. Geophys. Res. 106, 30645–30670. https://doi.org/10.1029/2001jb000179.

Rocchi, S., Armienti, P., D'Orazio, M., Tonarini, S., Wijbrans, J.R., Di Vincenzo, G., 2002. Cenozoic magmatism in the western Ross Embayment: role of mantle plume versus plate dynamics in the development of the West Antarctic Rift System. J. Geophys. Res., Solid Earth 107, 2195. https://doi.org/10.1029/2001jb000515.

Rocchi, S., Storti, F., Di Vincenzo, G., Rossetti, F., 2003. Intraplate strike-slip tectonics as an alternative to mantle plume activity for the Cenozoic rift magmatism in the Ross Sea region, Antarctica. Geol. Soc. (Lond.) Spec. Publ. 210, 145–158. https://doi.org/10.1144/gsl.sp.2003.210.01.09.

Rocholl, A., Stein, M., Molzahn, M., Hart, S.R., Wörner, G., 1995. Geochemical evolution of rift magmas by progressive tapping of a stratified mantle source beneath the Ross Sea Rift, Northern Victoria Land, Antarctica. Earth Planet. Sci. Lett. 131, 207–224. https://doi.org/10.1016/0012-821x(95)00024-7.

Salters, V.J.M., Stracke, A., 2004. Composition of the depleted mantle. Geochem. Geophys. Geosyst. 5. https://doi.org/10.1029/2003gc000597.

Seton, M., Müller, R.D., Zahirovic, S., Gaina, C., Torsvik, T., Shephard, G., Talsma, A., Gurnis, M., Turner, M., Maus, S., Chandler, M., 2012. Global continental and ocean basin reconstructions since 200 Ma. Earth-Sci. Rev. 113, 212–270. https://doi.org/10.1016/j.earscirev.2012.03.002.

Simmons, N.A., Forte, A.M., Boschi, L., Grand, S.P., 2010. GyPSuM: a joint tomographic model of mantle density and seismic wave speeds. J. Geophys. Res. 115. https://doi.org/10.1029/2010jb007631.

Sims, K.W.W., DePaolo, D.J., 1997. Inferences about mantle magma sources from incompatible element concentration ratios in oceanic basalts. Geochim. Cosmochim. Acta 61, 765–784. https://doi.org/10.1016/s0016-7037(96)00372-9.

Sims, K.W.W., DePaolo, D.J., Murrell, M.T., Baldridge, W.S., Goldstein, S., Clague, D., Jull, M., 1999. Porosity of the melting zone and variations in the solid mantle upwelling rate beneath Hawaii: inferences from ^{238}U–^{230}Th–^{226}Ra and ^{235}U–^{231}Pa disequilibria. Geochim. Cosmochim. Acta 63, 4119–4138. https://doi.org/10.1016/s0016-7037(99)00313-0.

Sims, K.W.W., Hart, S.R., 2006. Comparison of Th, Sr, Nd and Pb isotopes in oceanic basalts: implications for mantle heterogeneity and magma genesis. Earth Planet. Sci. Lett. 245, 743–761. https://doi.org/10.1016/j.epsl.2006.02.030.

Sims, K.W.W., Blichert-Toft, J., Kyle, P.R., Pichat, S., Gauthier, P.J., Blusztajn, J., Kelly, P., Ball, L., Layne, G., 2008. A Sr, Nd, Hf, and Pb isotope perspective on the genesis and long-term evolution of alkaline magmas from Erebus volcano, Antarctica. J. Volcanol. Geotherm. Res. 177, 606–618. https://doi.org/10.1016/j.jvolgeores.2007.08.006.

Sims, K.W.W., Pichat, S., Reagan, M.K., Kyle, P.R., Dulaiova, H., Dunbar, N.W., Prytulak, J., Sawyer, G., Layne, G.D., Blichert-Toft, J., Gauthier, P.J., Charette, M.A., Elliott, T.R., 2013. On the time scales of magma genesis, melt evolution, crystal growth rates and magma degassing in the Erebus volcano magmatic system using the ^{238}U, ^{235}U and ^{232}Th decay series. J. Petrol. 54, 235–271. https://doi.org/10.1093/petrology/egs068.

Sleep, N.H., 2006. Mantle plumes from top to bottom. Earth-Sci. Rev. 77, 231–271. https://doi.org/10.1016/j.earscirev.2006.03.007.

Storey, B.C., Leat, P.T., Weaver, S.D., Pankhurst, R.J., Bradshaw, J.D., Kelley, S., 1999. Mantle plumes and Antarctica–New Zealand rifting: evidence from mid-Cretaceous mafic dykes. J. Geol. Soc. (Lond.) 156, 659–671. https://doi.org/10.1144/gsjgs.156.4.0659.

Sun, S.S., Hanson, G.N., 1975. Origin of Ross Island basanitoids and limitations upon the heterogeneity of mantle sources for alkali basalts and nephelinites. Contrib. Mineral. Petrol. 52, 77–106. https://doi.org/10.1007/bf00395006.

Tappenden, V.E., 2003. Magmatic Response to the Evolving New Zealand Margin of Gondwana During the Mid-Late Cretaceous. PhD Thesis. University of Canterbury.

Timm, C., Hoernle, K., Werner, R., Hauff, F., van den Bogaard, P., White, J., Mortimer, N., Garbe-Schönberg, D., 2010. Temporal and geochemical evolution of the Cenozoic intraplate volcanism of Zealandia. Earth-Sci. Rev. 98, 38–64. https://doi.org/10.1016/j.earscirev.2009.10.002.

Trabant, C., Hutko, A.R., Bahavar, M., Karstens, R., Ahern, T., Aster, R., 2012. Data products at the IRIS DMC: stepping stones for research and other applications. Seismol. Res. Lett. 83 (5), 846–854. https://doi.org/10.1785/0220120032.

Watson, S., McKenzie, D., 1991. Melt generation by plumes: a study of Hawaiian volcanism. J. Petrol. 32, 501–537. https://doi.org/10.1093/petrology/32.3.501.

Watson, T., Nyblade, A., Wiens, D.A., Anandakrishnan, S., Benoit, M., Shore, P.J., Voigt, D., VanDecar, J., 2006. P and S velocity structure of the upper mantle beneath the Transantarctic Mountains, East Antarctic craton, and Ross Sea from travel time tomography. Geochem. Geophys. Geosyst. 7. https://doi.org/10.1029/2005gc001238.

Weiss, Y., Class, C., Goldstein, S.L., Hanyu, T., 2016. Key new pieces of the HIMU puzzle from olivines and diamond inclusions. Nature 537, 666–670. https://doi.org/10.1038/nature19113.

Willbold, M., Stracke, A., 2006. Trace element composition of mantle end-members: implications for recycling of oceanic and upper and lower continental crust. Geochem. Geophys. Geosyst. 7, 1–30. https://doi.org/10.1029/2005gc001005.

Workman, R.K., Hart, S.R., Jackson, M., Regelous, M., Farley, K.A., Blusztajn, J., Kurz, M., Staudigel, H., 2004. Recycled metasomatized lithosphere as the origin of the Enriched Mantle II (EM2) end-member: evidence from the Samoan Volcanic Chain. Geochem. Geophys. Geosyst. 5. https://doi.org/10.1029/2003gc000623.

Workman, R.K., Hart, S.R., 2005. Major and trace element composition of the depleted MORB mantle (DMM). Earth Planet. Sci. Lett. 231, 53–72. https://doi.org/10.1016/j.epsl.2004.12.005.

Zandomeneghi, D., Aster, R., Kyle, P., Barclay, A.H., Chaput, J., Knox, H., 2013. Internal structure of Erebus volcano, Antarctica imaged by high-resolution active-source seismic tomography and coda interferometry. J. Geophys. Res. 118, 1067–1078. https://doi.org/10.1002/jgrb.50073.

Zhao, D., 2007. Seismic images under 60 hotspots: search for mantle plumes. Gondwana Res. 12, 335–355. https://doi.org/10.1016/j.gr.2007.03.001.